Temperature gradients drive functional heterogeneity within muscle

Nicole T. George

A dissertation
submitted in partial fulfillment of the
requirements for the degree of

Doctor of Philosophy

University of Washington
2012

Reading Committee:
Thomas Daniel, Chair
Emily Carrington
Raymond Huey

Program Authorized to Offer Degree:
Biology

University of Washington

Abstract

Temperature gradients drive functional heterogeneity within muscle

Nicole T. George

Chair of the Supervisory Committee:
Professor Thomas L. Daniel
Department of Biology

During locomotion, muscles respond to an animal's varying need for speed, endurance, strength, and agility. Therefore, in addition to operating as motors, muscles also act as brakes, springs, and struts. Interestingly, if the physical, morphological, and neurological parameters determining muscle performance vary regionally, a muscle may actually concurrently operate with multiple functions. In this study, I investigated the functional consequences of an intramuscular temperature gradient, arising from the inevitable heat exchange between metabolic heat production and surface cooling.

In Chapter 1, I defined the determinants of muscle function and highlight the diverse roles muscles perform. I then discussed an emerging field, which shows that the factors determining muscle performance can regionally vary.

In Chapter 2 (George and Daniel, 2011), I characterized the temperature gradient throughout a muscle in the hawkmoth, *Manduca sexta.* I recorded multi-site temperature measurements during tethered flight and conducted isometric contraction tests to determine the effect of temperature on contractile dynamics. We found that the significant temperature gradient throughout the muscle will cause the warm region to contract with rapid individual twitches, while the cooler region will contract in unfused tetany.

In Chapter 3 (George et al., 2012), I determined how this temperature gradient affects regional mechanical power output. Work-loop methods, where muscle is cyclically lengthened and stimulated, allowed us to measure mechanical work. We found that the warm

region of muscle will produce positive power, thereby functioning as a motor. As temperature decreases, power output decreases, transitioning to negative values. Thus, the cooler region of muscle may serve a completely separate role, including that of a brake and/or spring.

In Chapter 4, I investigated if a temperature gradient additionally creates a locked-spring lattice, capable of storing and releasing energy, in the cool region of muscle. We used X-ray fiber diffraction to visualize the molecular dynamics of a contraction. A restrained lattice combined with reduced cross-bridge cycling in cool muscle indicates that cross-bridges are less able to detach from their binding sites. Thus, a temperature gradient likely forms a regional locked-spring lattice, whereby energy can be stored in the axial and radial extensions of cross-bridges.

TABLE OF CONTENTS

Page

List of Figures iii

List of Tables iv

Chapter 1: Introduction 1
1.1 Determinants of muscle power 2
1.1.1 Force-length relationship 2
1.1.2 Force-velocity relationship 3
1.1.3 Phase of activation 5
1.2 Functional diversity of muscles 5
1.2.1 Muscles that function as motors 6
1.2.2 Muscles that function as brakes 8
1.2.3 Muscles that function as springs 9
1.2.4 Muscles that function as struts 9
1.3 Functional heterogeneity within a single muscle 10
1.3.1 Variation in fiber type and architecture 10
1.3.2 Variation in fascicle strain 11
1.3.3 Variation in activation pattern and recruitment 12
1.4 Importance of functional heterogeneity 13

Chapter 2: Temperature gradients in the flight muscles of Manduca sexta imply a spatial gradient in muscle force and energy output 17
2.1 Abstract 17
2.2 Introduction 18
2.3 Materials and Methods 20
2.3.1 Moths 20
2.3.2 Temperature profiles 20
2.3.3 Force measurements 22
2.3.4 EMG measurements 23
2.3.5 Data acquisition 24
2.3.6 Statistical analysis 24
2.4 Results 25
2.4.1 Temperature profiles 25
2.4.2 Contractile rates 25
2.4.3 Extracellular evoked potentials 27
2.5 Discussion 32
2.5.1 Significant in vivo temperature gradient 32
2.5.2 No detectable regional specialization in contractile dynamics and neural activation 33
2.5.3 Temperature gradients induce mechanical gradients 34
2.6 List of symbols and abbreviations 36
2.7 Acknowledgements 36

Chapter 3: Temperature gradients drive mechanical energy gradients in the flight muscle of Manduca sexta 37
3.1 Abstract 37
3.2 Introduction 38
3.3 Materials and methods 42
3.3.1 Moths 42
3.3.2 Experimental apparatus and muscle preparation 42
3.3.3 Muscle length and strain 44
3.3.4 Muscle temperature 45
3.3.5 Phase of activation 45
3.3.6 Data acquisition 45
3.3.7 Statistical analysis 46
3.4 Results 46
3.4.1 Operating conditions 46
3.4.2 Effect of temperature on power output at the in vivo phase of activation 47
3.4.3 Subunit differences 50
3.4.4 Effect of phase of activation on the power–temperature relationship 52
3.5 Discussion 54
3.5.1 Temperature gradients within flight power muscles translate to functional gradients 55
3.5.2 Differences in physiology across the muscle do not compensate for temperature gradients 56
3.5.3 Implications for the role of different subunits in flight 57
3.5.4 Implications for locomotor control 58
3.5.5 Conclusions 60
3.6 List of abbreviations 60
3.7 Acknowledgements 60
Chapter 4: The cross-bridge spring: cool muscles store elastic energy 63
4.1 Abstract 63
4.2 Introduction 64
4.3 Results 68
4.3.1 Operating conditions 68
4.3.2 Effect of temperature on cross-bridge cycling dynamics 68
4.3.3 Effect of muscle location 70
4.4 Discussion 71
4.5 Material and methods 72
4.5.1 Moths 72
4.5.2 Work-loop preparation 72
4.5.3 X-ray diffraction 74
4.5.4 Diffraction pattern analysis 74
4.5.5 Data acquisition 75
4.6 Acknowledgements 76
Bibliography 77
Appendix A: Matlab code for Chapter 2 87
Appendix B: Matlab code to run work-loop experiment (Chapter 3 and 4) 91
Appendix C: Matlab code to analyze work-loop data (Chapter 3 and 4) 95

LIST OF FIGURES

Figure Number Page

1.1 Diagrammatic force-length and force-velocity relationship 4
1.2 Example work-loop traces 7
2.1 *Manduca sexta* preparation for force and electromyographic (EMG) measurement 21
2.2 Flight induces a significant temperature gradient across the DLM_1 26
2.3 Mean rise and fall times of a single isometric twitch as a function of temperature 28
2.4 Force plots of 25 Hz isometric contractions at 25, 30, 35 and 40ºC 30
2.5 Two simultaneously recorded EMG sequences from DLM_{1e} and DLM_{1a} 31
3.1 *Manduca sexta* preparation for the work-loop studies 40
3.2 Example positive, approximately zero, and negative work-loops 48
3.3 Power output plotted as a function of temperature for intact DLM_1 49
3.4 Mechanical power output of the dorsal subunits compared with the ventral subunits .. 51
3.5 The effect of phase of activation on power output with a temperature gradient 53
3.6 A schematic representation of a temperature-induced functional gradient 58
4.1 X-ray diffraction and work-loop preparation 66
4.2 Example work-loop traces and diffraction images from the hot and cold condition 67
4.3 Variation in lattice structure throughout the contraction cycle 69

LIST OF TABLES

Table Number Page

2.1 ANOVA *P*-values for the mean rise time, fall time, and time of peak force..... 29
2.2 Mean rise and fall times recorded from single isometric contractions 29
3.1 Mean power output for the *in vivo* phase of activation at 25, 30, 35, and 40ºC 49
3.2 Mean power output across the temperature gradient for all phases of activation..... 53

ACKNOWLEDGMENTS

My experience as a graduate student in the Daniel Lab has been incredible. Of course I must acknowledge that the entirety of this work would not have been possible without the extremely helpful mentorship of my advisor, Tom Daniel. Tom's unwavering optimism allowed me to see the bright side of every roadblock and his continued excitement gave me the drive needed to tackle each new project.

My committee members, Emily Carrington and Ray Huey, were also very generous with their time and expertise. Both Emily and Ray brought a refreshing perspective to my thesis and their feedback was instrumental in my efforts to communicate science to a broad audience.

Additionally, all the members of the Daniel lab have been very involved in my development as a scientist. They have been excellent role models, and the high standards they set have allowed me to continually improve. I would like to specifically thank Zane Aldworth, Armin Hinterwirth, Simon Sponberg, and Dave Williams. Their knowledge was kindly shared, and for that I am extremely grateful.

And finally I must thank my Mom, Dad and Sister, for their enduring support during graduate school. My family has always been there to comfort me, and more importantly, distract me with good food and good conversation. And last but not least, I must thank Aaron for his caring, kind, and patient nature. Frequently my nerves made me worry about meeting the many challenges along the way. Aaron provided the love and support needed to keep me calm and reassured that I could accomplish it all.

DEDICATION

To my mom and dad.

Chapter 1

INTRODUCTION

The motions executed by moving animals are incredibly diverse, ranging from the extreme sprint speeds of cheetahs, to the powerful jet propulsion used by squids, and large jump distances of kangaroos. Locomotion is a complex event, powered by the coordinated action of muscles. These muscles must respond to an animal's varying need for speed, endurance, strength, and agility. As such, muscles are separately suited for energy production, absorption, storage, and transmission. However, this division of labor may be considerably more complicated than previously thought. A single muscle can exhibit regional variation in the neurological and morphological parameters that determine mechanical performance, including muscle strain, fiber type, and activation pattern (Mu and Sanders, 2001; Pappas et al., 2002; Higham et al., 2008; English et al., 1993; Sponberg et al., 2011). Thus, in these cases, function within a single muscle may actually be heterogeneously distributed, with separate regions differently contributing to movement. By understanding the implications of regionally varying operating conditions, we will be better equipped to understand how muscles actuate dynamic locomotor behaviors.

Here we follow the functional consequences of an important, but overlooked, regionally varying parameter, the physiological environment in which the muscle operates. Given that a temperature gradient throughout an organism's musculature is an inevitable consequence of metabolic heat production paired with convective and radiative heat loss, the mechanical consequences of spatially varying temperature warrants further consideration. Because muscle contractile rates are temperature dependent, a temperature gradient may induce spatially specific, and functionally distinct roles throughout a single muscle. To introduce this concept of heterogeneous muscle function induced by a temperature gradient, this chapter presents the fundamentals of muscle mechanics and explores the diverse ways in

which muscles operate. I begin by reviewing the physical and physiological determinants of muscle force and power production. This is followed by an overview of the different ways muscles drive motion, acting as a motor, brake, spring, and strut. I will end by highlighting an emerging field in muscle research that investigates the complex concept of heterogeneous function throughout a muscle due to spatially varying operating conditions. As described below, our understanding of muscle function has become increasingly more detailed, with each development bringing us closer to a more realistic idea of how muscles control movement.

1.1 Determinants of muscle power

Force development in muscle contraction can be deceptively simple. The basic contractile unit of a muscle fiber is the sarcomere, which consists of interdigitating parallel thick and thin filaments, composed mostly of the protein myosin and actin, respectively. These filaments are arranged in a precise and repeated pattern such that they create a well-structured lattice. Cross-bridges, projecting from thick filaments bind to adjacent thin filaments. These cross-bridges then convert the chemical energy of ATP hydrolysis into mechanical work via conformational changes upon cross-bridge/actin binding and the release of a phosphate ion. When a muscle shortens, the repeated power stroke of several hundred active cross-bridges cause the overlapping thick and thin filaments to slide past each other (Alexander, 2003). However the ability of these contractile proteins to interact is complicated by both the spatial and temporal dynamics of force development. Because of these dynamics, morphological and neurological characteristics can greatly affect muscle performance. Extending from the idea of filament geometry and position dependent cross-bridge cycling, muscle performance is a function of its length, velocity, and activation characteristics.

1.1.1 Force-length relationship

Muscle force depends on the ability of cross-bridges to interact with actin binding sites, a trait directly attributable to myofilament overlap. Isometric contraction experiments on isolated fiber segments revealed the now classic length-tension relationship, demonstrating

muscle force is directly related to sarcomere length (Gordon et al., 1966). At the optimum sarcomere length for force production, myosin and actin filaments overlap such that the maximum number of cross-bridges are within binding range. At longer lengths force production declines due to reduced filament overlap and available binding sites. At shorter muscle lengths, thin filaments from the two halves of the sarcomere begin to overlap, resulting in obstructed binding sites and incorrect cross-bridge binding (Fig. 1.1A; Gordon et al., 1966). Not surprisingly, the actual relationship between length and tension depends, in part, on the specific lengths of the thin filaments in individual sarcomeres, a factor that markedly varies across species (Rassier et al., 1999; Walker and Schrodt, 1974).

1.1.2 Force-velocity relationship

Muscle has an approximate inverse relationship between force and shortening velocity: when muscle is stimulated and allowed to shorten under isotonic conditions, muscle velocity declines with increased loads, until a maximum load where muscle fibers can no longer shorten. In contrast, under increasing isotonic stretch conditions, muscle velocity continues to rise until approaching a yield point (Fig. 1.1B). This relationship between the force (F) and velocity (V) is well described by Hill's equation

$$(F + a) * (V + b) = (F_0 + a) * b$$

where F_0 is the isometric force produced, and a and b are constants that vary by individual muscle (Hill, 1938; McMahon, 1984; Alexander, 2003). Thus, there is a tradeoff between muscles that are particularly fast and muscles that generate large forces. Kier and Curtin (2002) determined the contractile properties for two differently specialized squid muscles, a muscle from the tentacles, suited for rapid prey capture, and a muscle from the arms, used in slow and forceful movements. As predicted, although maximum shortening velocity was ~10 times greater for tentacle muscle fibers, mean peak force was ~4 times greater for the low velocity arm muscle fibers (Kier and Curtin, 2002). The mechanical power output of a muscle is the product of its force and velocity. Thus, every point along the force-velocity curve has a corresponding power output value (Fig. 1.1B). Power output has a unique maximum at some intermediate velocity between 0 and the maximum shortening rate (Josephson, 1993; Alexander, 2003).

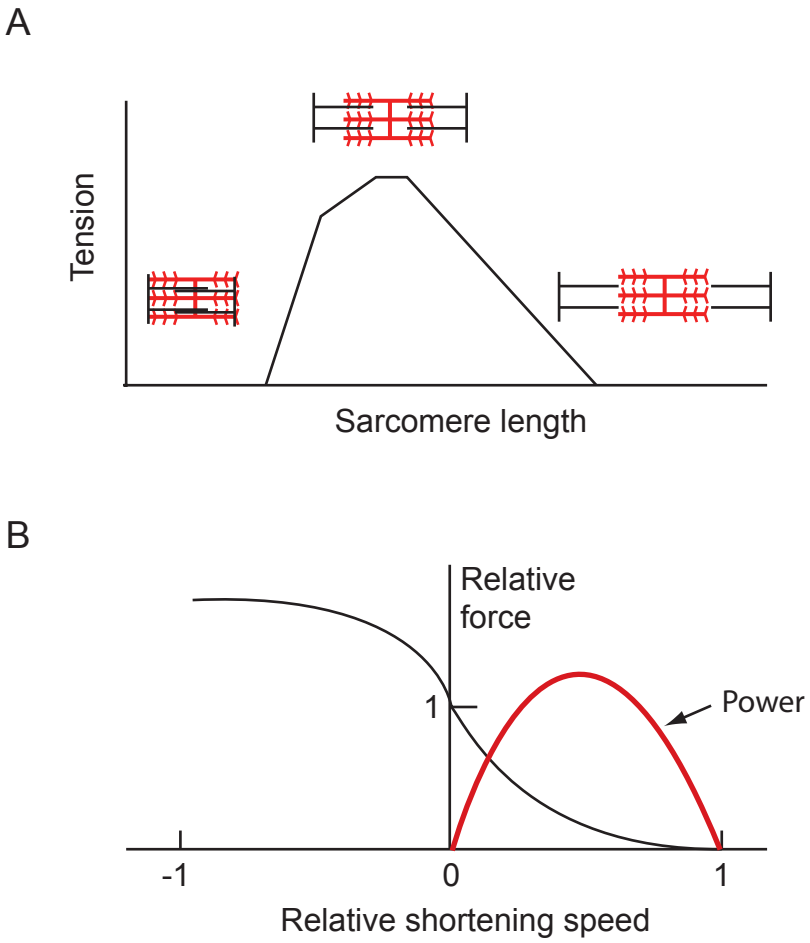

Figure 1.1: Diagrammatic force-length and force-velocity relationship. (A) The degree of myofilament overlap, and therefore available actin binding sites, dictates the maximum tension developed during a contraction. (B) Relative force as a function of shortening speed. Velocities greater than zero indicate muscle shortening, whereas velocities less than zero indicate muscle lengthening. Power output (represented by the red line) is the product of force and velocity. As such, maximum power output occurs at an intermediate velocity between 0 and maximum. Figures adapted from Alexander (2003).

1.1.3 Phase of activation

During the time course of muscle activation, force produced by the muscle rises rapidly following stimulation and then declines gradually during relaxation. As such, muscle activation characteristics, described by the timing, frequency, and rate of activation following stimulation, are additionally responsible for modifying power output and muscle performance. Varying the time at which activation occurs, commonly termed the phase of activation, can lead to significant differences in power output (Josephson, 1985; Stevenson and Josephson, 1990; Tu and Daniel, 2004b). In the hawkmoth *Manduca sexta*, advancing the phase of activation from 0.36 (during the lengthening phase) to 0.7 (during the shortening phase) actually reduces power output from maximal (~90 W kg^{-1}), to significantly negative, (~ –50 W kg^{-1}) (Tu and Daniel, 2004b). This variation in power output is the result of the previously described length-tension relationship, where force output varies with myofilament overlap.

In addition, the timing of a contraction, defined by the time to peak force and duration of relaxation, is essential in determining locomotor speeds. Internal fiber dynamics, including variation in cytoplasm Ca^{2+} levels, ATPase rates, and myofilament overlap, dictate a muscles contraction times. As with other biological rate processes, contractile rates also significantly depend on temperature. Both vertebrates and invertebrates benefit from the accelerated contractile rates associated with an increase in temperature (Josephson, 1984; Bennett, 1985; Swoap et al., 1993). For example, in the iliofibularis muscle of the lizard *Dipsosaurus dorsalis*, Swoap et al. (1993) measured a ~70% decrease in the time to peak tension with a 20ºC increase in temperature. Underlying this temperature dependence are the enzymatically catalyzed mechanisms associated with muscle contraction (Bennett, 1985). Decreased contraction times allow organisms to attain higher locomotor speeds and reaction rates, essential for high frequency cyclic motions such as synchronous insect flight and ballistic movements including escape maneuvers or prey capture.

1.2 Functional diversity of muscles

Although the aforementioned single contraction studies performed under constant length or

force conditions substantially advanced our understanding of the time course of force production in muscle, they fail to represent natural cyclic conditions and accurately predict muscle function *in vivo*. In order to replicate the natural kinetics and activation patterns of muscles used in oscillatory motions (e.g. flying, running, swimming), Josephson developed the work-loop method (Josephson, 1985). With this method, muscle is cyclically oscillated at physiological frequencies and strains under controlled muscle activation while simultaneously measuring force to calculate mechanical power output (Fig. 1.2). Work-loop studies have been instrumental in determining the functional consequences of various neural and mechanical determinants, including muscle strain, length, and phase of activation (Josephson, 1985; Stevenson and Josephson 1990; Johnson and Johnston, 1991; Swoap et al., 1993; Full et al., 1998; Rome et al., 1999; Tu and Daniel, 2004b; Donley et al., 2007). Ultimately, they have allowed us to begin to determine how muscles operate and function *in vivo* in a moving animal.

Until relatively recently, the classic assumption was that muscle produces only positive force while shortening, and thereby generates positive mechanical power output and operates as a motor. Because of this assumption, initial work-loop studies were performed under muscle strain, activation, and temperature conditions that maximized power output (Josephson, 1985; Stevenson and Josephson, 1990; Swoap et al., 1993). However, it was only until *in vivo* strain and activation conditions were used that a substantial diversity in power output and muscle performance was observed. We now know that muscles perform a broad range of specialized functions, including providing power for rapid motions, braking, storing and releasing energy, and aiding in energy transmission (Altringham et al., 1993; Marsh and Olson, 1994; Tu and Dickinson, 1994; Roberts et al., 1997; Full et al., 1998; Dickinson et al., 2000; Swank and Rome, 2001). A brief sampling of organisms below will highlight the diverse functions assigned to muscles in order to meet the fundamental demands of locomotion (for further review refer to Dickinson et al., 2000).

1.2.1 Muscles that function as motors

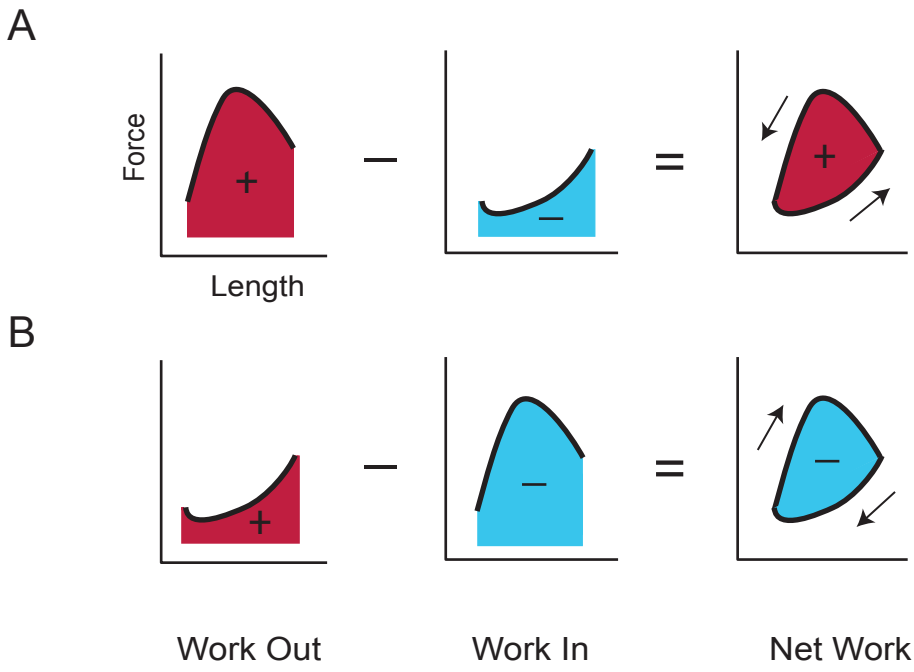

Figure 1.2: Example work-loop traces. Net work is the sum of work required to lengthen the muscle (work in) and the work returned by the muscle shortening (work out). (A) Muscles that function as motors produce positive power by developing force during the shortening phase. This corresponds with a counterclockwise work-loop. (B) A muscle that functions as a brake absorbs energy and produces force during the lengthening phase. Negative power output corresponds with a clockwise work-loop.

Muscles that operate as motors predominantly drive locomotion, including ballistic movements such as escape jetting by scallops and oscillatory motions such as wing movement in flight (Marsh et al., 1992; Biewener, 1998). These muscles generate force as they shorten and produce positive mechanical power throughout a contraction cycle (Fig. 1.2A). Power producing muscles are generally expected to have long parallel muscle fibers, a trait which allows them to create larger amplitude displacements as they shorten to move limb or body segments. For instance, in a comparison of two differently specialized muscles, Biewener (1998) measured extensively greater shortening in the muscle responsible for generating high mechanical power output, ~35% of the rest length versus 2% in the non-power producing muscle. Because the timing of muscle activation significantly affects power output, there is also a time dependent nature to muscle function. Muscles that generate positive mechanical power in rapid oscillatory movements require an early phase of activation in order to adequately develop force prior to the shortening phase of the cycle (Altringham and Johnston, 1990; Rome et al., 1993). This is exemplified by the power-phase curve of the dominant flight muscle of the hawkmoth. Maximal power output, ~90 W kg^{-1}, occurs when the muscle is activated ~6 ms before shortening, this is followed by a significant decrease, with power output actually transitioning to highly negative values shortly after shortening (Tu and Daniel, 2004b).

1.2.2 Muscles that function as brakes

Muscles may also produce negative power output, absorbing energy during the contraction cycle, and therefore function as a brake. In this case, muscles produce large forces during the lengthening phase of the cycle to actively slow limb or body segment movement. Unlike the characteristic counterclockwise work-loop of a power producing muscle, negative power output is indicated by a clockwise work-loop (Fig. 1.2B). In cyclic motions, such as in insect flight, muscles producing negative power can dampen oscillations that become unsteady. In addition, muscles that absorb work facilitate changes in motion requiring decelerations. Therefore, it appears that negative power output is essential in maintaining stability and control in locomotion. By modulating extrinsic factors such as the phase of activation and shortening velocity, the muscular system can selectively absorb energy when the mechanics

demand it. In the example of a running cockroach, select leg extensor muscles actually absorb energy (–19 W kg^{-1}) under *in vivo* stimulus and strain conditions (Full et al., 1998; Ahn and Full, 2002). Thus, in the cockroach leg there appears to be a division of labor, with some leg extensor muscles acting to extend the leg while others act as brakes to slow the leg during the swing phase and therefore stabilize motion.

1.2.3 Muscles that function as springs

Elastic energy savings is a crucial aspect of locomotion, allowing organisms to minimize their metabolic costs and increase efficiency. Although the sites of elastic energy storage are generally believed to be in non-muscular structures such as tendons and cuticle, muscle fibers can also act as springs to store and release energy (Alexander and Bennet-Clark, 1977; Alexander, 1984; Dickinson et al., 2005; Patek et al., 2011). This recoil energy could be stored in compliant cross-bridges and in the axial portions of the myofilament lattice. A recent study measuring changes in the muscle lattice structure using X-ray diffraction techniques, observed elastic deformation of thick filaments in asynchronous insect flight muscle (Dickinson et al., 2005). This elastic stretch and recoil of the myosin filaments suggests that a portion of energy storage takes place within the myofilaments themselves. Elastic energy stored in stretched muscle filaments and cross-bridges at the end of one phase of the contraction cycle would be released during the second phase, passively contributing to reduce the total energy requirements of locomotion.

1.2.4 Muscles that function as struts

Lastly, muscles can also serve as struts, stiffening to play a force-transmitting role. These muscles are commonly short and pinnate, allowing them the ability to generate large forces with little change in length. The well-described force-velocity curve highlights this tradeoff between work rate and force output (Hill, 1938). By operating isometrically (v = 0), strut-like muscles transfer energy from one part of the body to another and can also function in series with tendons to store and recover energy. In turkeys, for example, the isometrically contracting lateral gastrocnemius muscle functions as a strut, transferring energy to the spring-like tendon, which stretches and recoils to provide 60% of the work needed to move

the body up and down (Roberts, 1997). In fish, muscle function can actually vary based on the timing of muscle activation with respect to the bending wave traveling across the body during undulatory swimming. It appears that early in the cycle, the anterior muscle shortens to produce positive power. Later in the cycle, and further along the body position, the muscle becomes stiff and passively transmits power to the tail fin, where the majority of the hydrodynamic forces are generated (Altringham and Ellerby, 1999).

Taken together, the literature suggests that muscles can perform a range of functions. However, the division of labor may not be as simple as is commonly believed. As I discuss below, recent evidence suggests that physiological parameters may actually vary within a single muscle, indicating that a muscle has the ability to perform multiple tasks simultaneously.

1.3 Functional heterogeneity within a single muscle

Recent studies observing regional variation in morphological and neurological *in vivo* operating conditions within a single muscle have revealed an added level of complexity to muscle function and performance. Researchers have observed spatially varying fiber architecture (Mu and Sanders, 2001; Wang and Kernell, 2001), segment strain (Pappas et al., 2002; Ahn et al., 2003, Higham et al., 2008, Higham and Biewener, 2008), and motor recruitment (English et al., 1993; Holtermann et al., 2005; Wakeling, 2009) in a range of animals, from vertebrates to invertebrates. Because these parameters greatly affect the mechanical properties of muscle, they have significant implications for how a single muscle operates. The concept of heterogeneously distributed operating conditions raises the notion of a muscle comprising of a series of components that operate with distinct functions. Understanding this complexity will influence our view on how muscles cooperate to produce controlled and coordinated motion.

1.3.1 Variation in fiber type and architecture

Muscles commonly meet the diversity of motor activities required with fibers differentially

suited for power, speed, and endurance. These fibers can have significantly different contractile dynamics and biochemical composition. Thus, the architectural design of a motor unit will greatly influence muscle function and performance. Interestingly, numerous studies have observed fiber segregation within a single muscle, suggesting heterogeneous fiber composition may be a general property of intramuscular organization (Monti et al., 2001; Mu and Sanders, 2001; Wang and Kernell, 2001).

For instance, several vertebrates similarly exhibit a proximo-distal gradient of Type I, slow oxidative, to Type II, fast oxidative, fibers in a lower hindlimb muscle (Wang and Kernell, 2001). Presumably this gradient in fiber type will lead to differential force generation, with the slow oxidative fibers, located deep within the muscle, recruited prior to the superficial fibers. As a result, force will be transmitted from the active fibers to the distal passive fibers, which will act as a compliant structure and affect the overall mechanics of the muscle (Monti et al., 2001). In a comparison of a homologous hindlimb muscle of three vertebrates, the proximo-distal fiber type gradient varied, suggesting that heterogeneous fiber distribution may be tuned for the specific needs of the organism (Wang and Kernell, 2001).

In addition, if compartments of a muscle can be separately activated (discussed further below), fiber type regionalization could elicit heterogeneous functional output. In humans, the inferior pharyngeal constrictor muscle (IPC; involved in swallowing, respiring, and vocalizing) consists of a caudal and rostral compartment composed mainly of slow twitch or fast twitch fibers, respectively. This segregation indicates the IPC may serve two functions, with the caudal region involved in continually preventing air from entering the esophagus during inspiration, and the rostral region involved in the rapid and powerful movement required when swallowing (Mu and Sanders, 2001). Although the full implications have yet to be realized, it appears that heterogeneous fiber composition permits the muscular system the ability to tune the mechanical actions of a muscle to the various functions required.

1.3.2 Variation in fascicle strain

It is often assumed that when a muscle contracts, the fibers throughout the muscle shorten uniformly. However, because of differences in fiber architecture and the mechanical

properties throughout a muscle (e.g. tendon attachment), segment shortening can actually be nonuniform. As a consequence of the relationship between force output and muscle length, variable fascicle strain within a muscle will also induce heterogeneous motor output.

Utilizing techniques such as magnetic resonance imaging and sonomicrometry, several recent studies measured the *in vivo* strain patterns of several segments throughout a muscle during natural movement (Pappas et al., 2002; Ahn et al., 2003, Higham et al., 2008, Higham and Biewener, 2008). In the semimembranous muscle of American toads, the distal segment strains differently than the central and proximal segment during *in vivo* hopping. Not only does the distal segment shorten less than the rest of the muscle, but it also has a more varied pattern, with the distal segment actually lengthening slightly before shortening during a hop (Ahn et al., 2003). When these muscle segments are simultaneously activated, they will operate at different points of their force-length and force-velocity relationships. As such, they will ultimately produce and absorb variable amounts of mechanical energy. In one study by Higham and Biewener (2008), variable strain resulted in the distal region of the medial gastrocnemius muscle of the guinea fowl producing ~4 times less power than the proximal region. While the exact causes of this regionalized strain require further investigation, likely factors include varying stiffness caused by nonuniform aponeurosis association, asymmetries in muscle architecture, and inhomogeneities in fiber type (Ahn et al., 2003; Higham and Biewener, 2008; Azizi and Roberts, 2009).

1.3.3 Variation in activation pattern and recruitment

The degree and timing of muscle activation relative to the length cycle significantly affects mechanical power output. Although it is generally assumed that simultaneous activation occurs within a muscle, the ability for spatially distinct activation would afford the organism an increase in control and efficiency. Not surprisingly, numerous organisms show muscle compartmentalization, the phenomenon where a muscle is organized into anatomical compartments, each with their own primary nerve branch (Hoffer et al., 1987; English et al., 1993; Scholle et al., 2001).

The ability for the preferential recruitment of muscle fibers permits mechanical partitioning and can lead to regionally distinct neuromechanical function within a single

muscle (Scholle et al., 2001; Holtermann et al., 2005; Higham et al., 2008; Wakeling, 2009). In the triceps brachii muscle of rats, electromyographic recordings from an array of surface electrodes demonstrate a selective shift in activation throughout a gait cycle, with separate regions of the muscle activated prior to ground contact and during the stance phase (Scholle et al., 2001). These results suggest that neuromuscular compartments may serve as an organizational tool for allocating functional roles within a muscle. Interestingly several studies noted instances where the pattern of variation in activation was sensitive to mechanical demand, indicating the nervous system may actively select the heterogeneous output (Holtermann et al., 2005; Higham et al., 2008; Wakeling, 2009). Overall, these details highlight the complexity of muscle and demonstrate the potential for context dependent multifunctional output.

1.4 Importance of functional heterogeneity

Although it is becoming clear that a muscle can be comprised of separately functioning components, the actual importance of this regional variation has yet to be fully understood. Presumably, differential activation suggests that muscle performance can be tuned, with the ability to change power output in response to demand almost immediately (Sponberg and Daniel, *in prep*). In addition, variable mechanical actions produced around a single joint by regional strain differences within a single muscle suggest increased control over joint mechanics. Also, variable fiber type and architecture with separate force-length relationships (and therefore different optimal lengths for force generation) implies a greater force-length plateau and a more generalized, broad ranging muscle. Within-muscle heterogeneity may be a common feature of vertebrates and invertebrates that enables muscles to operate more efficiently over a range of locomotor behaviors. As such, this added level of complexity should be further pursued in order to fully understand the connection between muscle physiological conditions and biomechanical performance.

In the work that follows, I expand upon these fundamental issues, addressing an important, yet overlooked, aspect of muscle heterogeneity. Despite growing evidence that functional heterogeneity may occur within regions of a muscle because of morphological or neurological differences, the role of the physiological environment in which the muscle

operates has generally not been considered. During muscle contraction, heat is produced as chemical energy is converted into mechanical work. As of yet, the temperature gradient that inevitably forms within a system due to metabolic heat production paired with convective and radiative heat loss has largely been ignored. Because the contractile rate processes of muscle show a strong thermal dependence, a temperature gradient could greatly influence both the temporal and spatial dynamics of muscle force generation and power production.

Therefore, in Chapter 2, I investigated three important aspects of temperature dynamics in the dominant flight muscle, the dorsolongitudinal muscle (DLM_1), of the hawkmoth *Manduca sexta* (George and Daniel, 2011). I first determined that there was indeed a significant difference in the spatial distribution of temperature across the five subunits of the DLM_1 during tethered flight, with the outermost dorsal DLM_1 subunit being significantly cooler than the innermost ventral DLM_1 subunit. Secondly, our data from isometric contraction tests confirm that the contractile dynamics of the DLM_1 are indeed temperature dependent, with lower temperatures resulting in reduced contraction rates. Thirdly, I recorded simultaneous electromyograms from separate muscle bundles to compare the fine scale neural activation timing. The separately innervated muscle bundles do not appear to employ a spatial offset in timing to correct for the thermal gradient and therefore the induced force generation gradient that arises during flight. This suggests a temperature gradient will necessarily result in a subsequent mechanical energy gradient traveling from the innermost DLM_1 to the outermost DLM_1 subunit.

In Chapter 3 (George et al., 2012), I further examined the functional consequences of an intramuscular temperature gradient with a temperature controlled work-loop study. With this technique, I measured how mechanical power output varies throughout a muscle in response to a temperature gradient. Results show that the total amount of work produced by the DLM_1 significantly decreased as temperature decreased, even transitioning to significantly negative values. Warmer ventral subunits that produce positive power will behave as a motor, whereas cooler dorsal subunits producing zero to negative power will presumably act as a damper and/or elastic energy storage source. Thus, although muscles are classically thought to function solely as a motor, spring, brake, or strut, it appears that they may actually concurrently operate with an array of functions as a consequence of an internal temperature gradient.

The concept that a temperature gradient could allow regions of a muscle to aid in elastic energy storage is particularly interesting. Several studies have concluded that elastic energy storage is crucial for insect flight, allowing insects to greatly reduce the inertial power costs of accelerating the wings (Alexander and Bennet-Clark, 1977; Ellington, 1984; Dickinson and Lighton, 1995). Although it is generally assumed that the main site of energy storage is in resilin within the cuticle, we would like to suggest that a temperature gradient provides another mechanism by which energy could be stored. Cross-bridges of the cooler region of muscle, with their reduced cycling rates, would remain on average more attached to the thin filaments. This would create a stable region in the muscle that could behave as a locked-spring lattice, where the cross-bridges and myofilaments could serve as springs, storing and releasing energy.

In Chapter 4 of my thesis, I sought to find molecular evidence for the temperature dependence of cross-bridge cycling and their role in energy storage using time-resolved small-angle X-ray fiber diffraction methods. With this technique, I was able to monitor the movement of cross-bridges at the needed spatial and temporal scale in hot and cold muscle under *in situ* cycling conditions. Variation in the diffraction patterns throughout a contraction revealed significantly temperature dependent cross-bridge cycling dynamics. Although warm muscle showed the expected fluctuation in cross-bridge mass distribution, cold muscle showed stable non-cycling cross-bridge activity, in addition with an overall restrained lattice spacing. Taken together, these findings suggest that in the cooler region of the DLM_1, a percentage of cross-bridges remain bound throughout the cycle leading to a locked-spring lattice capable of storing and releasing energy. Overall, this novel concept of heterogeneous muscle function and an energy storing locked-spring lattice induced by a temperature gradient has significant implications for the complexity of muscle function and energy saving mechanisms.

Because temperature gradients are the inevitable consequence of internal energy generation and heat dissipation, this form of functional heterogeneity may be a general phenomenon of locomotor systems. Thus, although the implications of functional heterogeneity are still poorly understood, it is clear that accounting for a temperature gradient will be necessary in order to understand how muscles meet the varying requirements of locomotion.

Chapter 2

TEMPERATURE GRADIENTS IN THE FLIGHT MUSCLES OF *MANDUCA SEXTA* IMPLY A SPATIAL GRADIENT IN MUSCLE FORCE AND ENERGY OUTPUT

Nicole T. George and Thomas L. Daniel

J Exp Biol, 2011

DOI: 10.1242/jeb.047969

2.1 Abstract

There is a significant dorso-ventral temperature gradient in the dominant flight muscles [dorsolongitudinal muscles (DLM_1)] of the hawkmoth *Manduca sexta* during tethered flight. The mean temperature difference was 5.6ºC (range=3.8-6.9ºC) between the warmer, ventral-most and the cooler, dorsal-most subunits. As force generation in muscle depends on temperature, the mechanical energy output of more dorsal subunits will differ from that of deeper and warmer muscle subunits. To test this hypothesis, we isolated the dorsal subunits and the ventral subunits and recorded both single and 25 Hz (wingbeat frequency) isometric contractions at a range of temperatures. Our data show that the contractile dynamics of the various regions of the DLM_1 are similarly affected by temperature, with higher temperatures leading to reduced contraction times. Furthermore, using standard electromyography, we showed that the different regions are activated nearly simultaneously (mean time difference=0.22 ms). These observations suggest that the existence of a temperature gradient

will necessarily produce a mechanical energy gradient in the DLM_1 in *M. sexta.*

2.2 Introduction

As with other biological rate processes, muscle function is strongly influenced by temperature. Specifically, muscle contraction rates (the rates of both force development and relaxation) are accelerated by an increase in temperature in both invertebrates and vertebrates (Josephson, 1984; Bennett, 1985). Work-loop studies, which measure the force produced by muscle while lengthening and shortening, have demonstrated that the mechanical power, or work output, of muscle increases as temperature increases (Stevenson and Josephson, 1990; Josephson, 1999). Biologically relevant ranges of *in vivo* temperature can therefore have significant impacts on locomotor performance.

Many animals achieve elevated muscle temperatures via endogenous heat production during muscle contraction (Heinrich, 1995). This heat production follows from the inherent inefficiency of muscle, with only ~5-9% of the chemical energy appearing as mechanical work and the rest released as heat (Ellington, 1985; Josephson and Stevenson, 1991). In several large insects, this heat byproduct leads to elevated thoracic temperatures that are well above ambient temperatures (Heinrich, 1974). Because the contractile rates of these muscles are temperature dependent, increased muscle temperature due to endogenous heat production allows these insects to increase their wingbeat frequency and thus produce greater mechanical power output (McCrea and Heath, 1971).

Previous studies of insect thermoregulation assumed that temperature is spatially uniform throughout the thoracic flight muscles, and therefore assessed temperature at only one spatial location. Although such methods provide valuable insight into operating thoracic temperatures in freely flying insects, they do not reveal any spatial variation in temperature (Heinrich, 1971; Heinrich and Casey, 1972; Janiszewski, 1984; Coelho, 1991). Such variation, however, is a probable consequence of metabolic heat production paired with dorsal convective cooling and ventral insulation surrounding the flight musculature. Given the strong thermal dependence of muscle function and the increased core temperature insects generate, we chose to examine the possibility of thermal inhomogeneity within flight muscle. Unless compensated for, any spatial gradient in temperature that arises because of

endogenous heat production necessarily creates spatial gradients in mechanical and energetic performance. This potential effect is particularly relevant to animals with large muscles that span a significant percentage of the body area and are aligned such that some sub-regions are located near the surface and others near the central axis. Consequently, cooler muscles near the surface could have dramatically different contraction dynamics than hotter, more centrally located muscles.

Here we document a temperature gradient and its possible functional consequences in the flight muscles of *Manduca sexta*, a large, active hawkmoth. Specifically, we address how the activation and contraction dynamics throughout an insect's flight muscle vary due to regional temperature differences that arise from the spatial distribution of heat production and heat loss mechanisms. *M. sexta* generates a highly elevated thoracic temperature (~40-43ºC maximum, ~15-25°C above ambient temperature) during free flight (Heinrich and Casey, 1972). The dominant flight muscles of *M. sexta* —the dorsolongitudinal muscles (DLM_1) (*sensu* Kondoh and Obara, 1982)— power the down-stroke of the wings and occupy the majority of the mesothorax. The flight muscles of *M. sexta* are synchronous muscles, with a single muscle action potential eliciting each contraction, in contrast to the asynchronous flight muscles of Diptera and other insects (Kammer, 1968). While activation is synchronous with wing beats, it is not known whether the timing of the activation of the subunits is simultaneous or phase-shifted.

If the DLM_1 subunits have similar contractile dynamics and are simultaneously activated, a temperature gradient will likely result in warm, ventral subunits producing isolated twitches whereas the cooler, more dorsal subunits, with their slower contraction dynamics, may remain in unfused tetany. These temperature-induced contractile differences could indicate an associated gradient in mechanical power output throughout the DLM_1. Such a concept could have significant implications for muscle efficiency and overall animal locomotor performance. In this study, we address three related questions. First, does temperature vary spatially throughout the flight muscles? Second, are the DLM_1 regionally specialized to compensate for the temperature-induced differences in contraction dynamics? Third, are muscle subunits activated independently in order to correct for a temperature-induced offset in the time of peak force?

2.3 Materials and methods

2.3.1 Moths

Manduca sexta (Linnaeus 1763) were obtained from a colony maintained by the Department of Biology at the University of Washington, Seattle, WA, USA. Moths were used within 5 days of eclosion. Prior to use, moths were maintained at 4°C for up to one day to immobilize them.

The DLM_1 are composed of five subunits —$DLM_{1a\text{-}e}$— that run longitudinally along the length of the mesothorax and attach to the cuticle at the first and second phragmata (Fig. 2.1A) (Tu and Daniel, 2004a). Each DLM_1 subunit is ~1 mm thick and is separately innervated by neurons in the IIN_{1C} nerve (Kondoh and Obara, 1982; Eaton, 1988).

2.3.2 Temperature profiles

We chose to measure the temperature profiles of the DLM_1 during tethered flight because our constraints of multi-site and continuous measurement made free flight recording problematic. Temperature of the DLM_1 subunits was measured to the nearest 0.1ºC using a copper-constantan thermocouple embedded into a 30 gauge hypodermic probe (HYP-1, Omega Engineering Inc., Stamford, CT, USA). The voltage output from this probe was relayed to a central processing unit. To verify the spatial resolution of the probe, we measured the temperature of well-mixed 49ºC water within a beaker set in an air stream of 22ºC. After detecting the initial temperature difference at the surface layer, the probe measured a constant 49ºC throughout the water. This indicates that the thermocouple measures temperature at the tip of the probe rather than spatially averaging temperature along the distal needle. This probe was attached to a micromanipulator such that it could be positioned in any of the muscle subunits. A 10-turn 5K Potentiometer (International Resistance Co., St Petersburg, FL, USA), attached to the pinion of the vertical drive of the micromanipulator, was used to monitor the thermocouple's position throughout the DLM_1. The probe was inserted through a small hole cut in the cuticle of the mesothorax to the right of the midline. Scales on the dorsal thoracic plates obscured the insertion point, and so were removed. Moths were ventrally

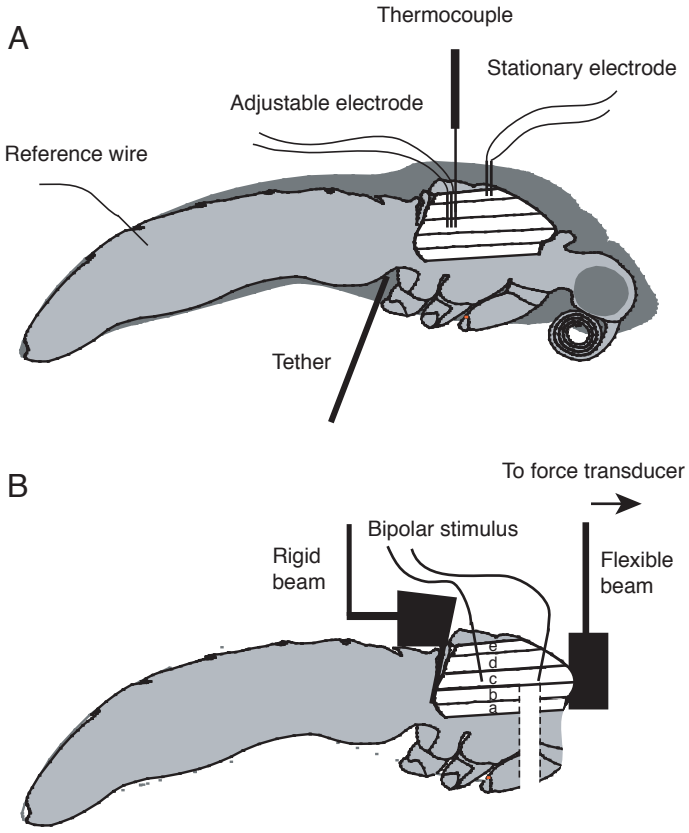

Figure 2.1: *Manduca sexta* preparation for force and electromyographic (EMG) measurement. (A) We recorded simultaneous EMGs during tethered flight from a stationary electrode in DLM_{1e} and an adjustable electrode in all other DLM_1 subunits. The temperature of each subunit was measured with a thermocouple probe. The dark gray outer layer represents the insulative fur covering the body of *M. sexta*. (B) After removing the moth's head, wings, legs, and scales, we secured the mesothorax between a rigid posterior grip and a flexible anterior grip attached to a force transducer. A thin circumferential cut was then made around the mid-mesothoracic cuticle to isolate the DLM_1 between the two grips. The DLM_1 subunits were either left intact or the dorsal ($DLM_{1c–e}$) or ventral subunits (DLM_{1ab}) were isolated. Muscles were stimulated with supramaximal stimuli to induce either single isometric twitches or 25 Hz contractions. Figure adapted from Tu and Daniel (Tu and Daniel, 2004a).

tethered to a brass rod that was set just posterior to the metathoracic legs. The rod was fixed in place with a mixture of cyanoacrylate and sodium bicarbonate powder. After a 10 min recovery period, moths were induced to fly with a constant airstream and occasional gentle probing. Individuals that did not exhibit continuous flight for at least 10 min were excluded from analysis. Upon initiation of flight, we lowered the probe through the DLM_1 in ten 0.5 mm increments, roughly half the thickness of an individual subunit. Each 'scan' of the DLM_1 took less than 20 s, and we repeated this scan every minute that the moth flew (N=10 moths).

To assure ourselves that removal of the dorsal thoracic scales did not significantly alter the temperature difference between the DLM_1, we conducted two independent tethered-flight temperature measurements. We first tested moths with the dorsal scales in place. Then, after a 10 min rest period, we removed the scales on the same moth and repeated the temperature scan. Because these experiments were performed as a quick approximation to verify that dorsal scales did not significantly alter the temperature gradient, we measured temperature only to the nearest degree using a digital multimeter (N=4 moths).

2.3.3 Force Measurements

We assessed the effect of temperature on the isometric contractile dynamics to determine if there was regional specialization for temperature sensitivity on force production in each of the subunits comprising the DLM_1. We adapted the protocol established by Tu and Daniel (Tu and Daniel, 2004a) for DLM_1 isolation and force measurement. To facilitate access to the thoracic muscles, we removed the head, wings, legs, and scales covering the dorsal and ventral surface. The DLM_1 were isolated between two grips attached to micromanipulators: a posterior fixed grip inserted into the groove beside the second phragma. The anterior was connected to a rigid lever force transducer (FORT250, WPI, Sarasota, Florida, USA). The force signal was passed through a bridge amplifier (Measurements Group, Chapel Hill, NC, USA).

A strip of acetate transparency film was glued across the two grips and then cut down the middle. This method serves as a positioning guide to prevent any change in length or shape of the thorax (Tu and Daniel, 2004a). We then excised a thin strip of cuticle near the anterior grip to mechanically isolate the thoracic muscles. Using the micromanipulators, we

repositioned the apparatus such that the acetate strips were aligned, returning the thorax to its original position.

To assess any regional specialization for contractile performance, we measured isometric force in three different preparations: (1) intact DLM_1 comprising all five subunits, (2) DLM_1 in which the ventral subunits ($DLM_{1a,b}$) were removed, leaving only the dorsal DLM_1 ($DLM_{1c–e}$; Fig. 2.1B) and (3) DLM_1 in which the dorsal subunits ($DLM_{1c–e}$) were removed, leaving the ventral subunits intact ($DLM_{1a,b}$).

To regulate the temperature of the muscle, we immersed the entire thorax in a temperature-controlled bath of *M. sexta* saline (Lei et al., 2004). An immersion circulator was used to heat water piped through an aluminum stage on which a Petri dish of this saline rested (Haake DC3, DM Scientific, Houston, TX, USA). The solution was then heated to 25, 30, 35 and 40°C to encompass the possible range of free-flight temperatures (Heinrich, 1974). To deliver supramaximal stimuli, a homemade stimulator was connected to two minuten pins that were inserted through the posterior and anterior notum along the same longitudinal transect of the DLM_1. Stimuli were either square pulses (0.2 ms long, for single contractions) or a train of pulses at 25 Hz to elicit contractions at wingbeat frequency. We recorded the evoked potential with a differential electrode placed in the DLM_1 near the posterior grip (N=5 moths per DLM_1 group, with five single isometric contractions or 10 25 Hz contractions per moth). Rise time is defined as the time required for tension to develop from 10% of peak tension to peak tension, and fall time is the duration of time required to return to 10% of peak tension.

2.3.4 EMG measurements

We used electromyographic (EMG) measurements to quantify the timing and any phase delays in activation of the five subunits. This allowed us to examine whether there are any clear neural correlates in the timing of muscle contraction peaks at different temperatures. EMGs were recorded from tethered moths that had sustained wing beating for at least 10 min. Regional EMG timing measurements were accomplished with one electrode fixed in the dorsal-most subunit, DLM_{1e}, and a second electrode was attached to a micromanipulator such that it could be lowered through the DLM_1. This allowed us to evaluate the variation in

activation timing between simultaneous signals from any DLM_1 subunit and from DLM_{1e} (N=10 moths, ~20 spikes per moth). In addition, a thermocouple was attached to the adjustable electrode to measure concurrent temperature profiles.

The electrodes were made of insulated insect pins soldered to 0.051 mm diameter stainless steel wires, insulated with Teflon® to a diameter of 0.114 mm (A-M Systems, Sequim, WA, USA). The stationary electrode was placed in DLM_{1e} to the right of the midline. The adjustable electrode was then inserted posterior to the stationary electrode. A common reference wire was inserted into the abdomen (Fig. 2.1A). The signals were amplified (x1000) with a differential AC amplifier (model 1800, A-M Systems) and band-pass filtered (300-20kHz).

EMGs were analyzed using custom peak detection software in MATLAB (The MathWorks, Natick, MA, USA) developed by M. S. Tu (University of Washington, Seattle, WA, USA) to determine the relative time difference of paired muscle subunits for which there were concurrent recordings.

2.3.5 Data Acquisition

Muscle temperature, probe position, force measurements, and extracellular evoked potentials were sampled at 5000 Hz with a data acquisition system (USB-1408FS, Measurement Computing, Norton, MA, USA).

2.3.6 Statistical Analysis

Variables, such as rise and fall time, were first averaged across trials to give means for each individual. Results and statistical tests for each experimental condition are reported as means across individuals. To evaluate the temperature-dependent response of these variables and the differences among subunit groups, we used ANOVA and Tukey–Kramer honestly significant difference (HSD) tests. Because we cannot assume the normality of our data, we confirmed our ANOVA with nonparametric Wilcoxon tests. Results from these tests did not lead to conflicting statistical conclusions. Data are presented as means ± s.e.m. unless otherwise indicated.

2.4 Results

2.4.1 Temperature profiles

The spatial patterns of temperature throughout the DLM_1 were recorded every minute that a moth flew, starting with the initiation of low-amplitude wing movement to encompass the warm-up period. At least 10 min of flight were required for analyses. Mean ambient temperature during flight trials was 21.3±0.6°C (s.d.). All trials showed a significant temperature gradient in the dorso-ventral direction (Fig. 2.2A,B). When calculating the mean temperature of each subunit across all individuals, we excluded the first 5 min of warm-up flight. DLM_{1e} (the dorsal-most subunit) was the coolest; on average only 2.4±0.6ºC above ambient temperature. Each subunit was progressively warmer in the ventral direction, with DLM_{1a} 8.0±0.7ºC above ambient temperature (ANOVA, $P<0.0001$; Fig. 2.2B). Though each neighboring subunit did not differ statistically, DLM_{1a} was statistically different from DLM_{1e} and DLM_{1d} (Tukey–Kramer HSD, $P<0.05$). The two most extreme subunits, DLM_{1a} and DLM_{1e}, had a mean temperature difference of 5.6±0.3ºC, with a maximum temperature difference of 8.3ºC (*t*-test, $P<0.0001$).

Similar to the trials without dorsal scales, moths with intact scales maintained a significant mean temperature difference of 6±1ºC between the outer DLM_1 after a 5 min warm-up period (*t*-test, $P<0.01$). However, the mean temperature of each subunit was elevated in comparison to the scale-removed trial. The mean temperature difference of DLM_{1e} and DLM_{1a} from the ambient temperature was 8±1ºC and 15±1ºC, respectively. The dorsal scales were then removed and the moth was induced to fly again. In these trials, moths maintained a slightly lower temperature difference between the outermost DLM_1 subunits of 5±1ºC (*t*-test, $P<0.05$).

2.4.2 Contractile rates

The temperature dependence of muscle contractile rates was analyzed for the intact DLM_1 and two groups of subunits: $DLM_{1a,b}$, and $DLM_{1c–e}$. Muscles were electrically stimulated to induce both single contractions and 25 Hz contractions.

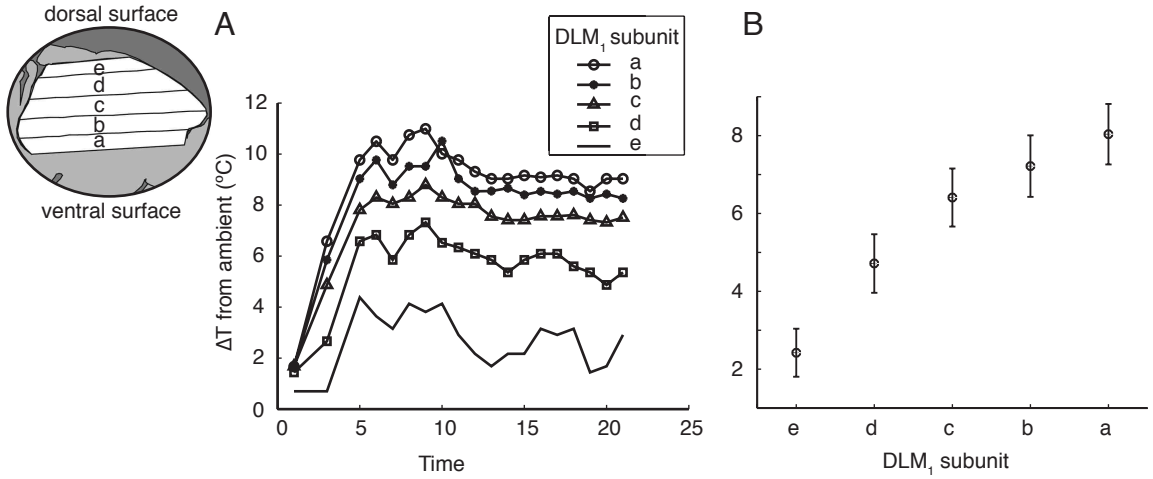

Figure 2.2: Flight induces a significant temperature gradient across the DLM_1 in the dorso-ventral direction. (A) A temperature profile from an individual moth during tethered flight is plotted against time. The temperature difference (ΔT) from ambient (21.8ºC) of each DLM_1 subunit is represented by a separate line. After a warm-up period of ~5 min, a fairly constant and distinct temperature was maintained by each subunit. (B) Mean ΔT from ambient of each subunit across all individuals after a 5 min warm-up period (N=10 moths). The mean temperature of each subunit significantly increased in the ventral direction (ANOVA, $P<0.0001$). Although neighboring subunit temperatures were not statistically different, DLM_{1a} was statistically different from DLM_{1e} and DLM_{1d} (Tukey–Kramer HSD, $P<0.05$). Values reported as means ± s.e.m.

For both rise times and fall times from 25 to 35ºC, we found no statistical difference between our two subunit groups, $DLM_{1c–e}$ and $DLM_{1a,b}$ (ANOVA, $P>0.1$; Fig. 2.3 and Table 2.1). There was, however, a significant difference in the rate of relaxation between these two groups at 40ºC (ANOVA, $P<0.05$).

Consistent with prior studies (Bennett, 1984; Josephson, 1984; Langfeld et al., 1989; Johnson and Johnston, 1990; Swoap et al., 1993) an increase in temperature led to significantly reduced contraction rise and fall times (ANOVA, $P<0.05$; Fig. 2.3 and Table 2.2). Although none of the increases in temperature led to a significant pairwise difference in rise and fall times, we did find statistically significant differences across trials separated by 10ºC or more (Tukey–Kramer HSD, $P<0.05$). From 25ºC to 35ºC, the mean rise times of $DLM_{1c–e}$ and $DLM_{1a,b}$ combined decreased by 31.9% whereas mean fall times decreased by 36.6%.

In all three experimental groups, muscles subject to the wingbeat stimulation frequency of 25 Hz exhibited full relaxation between subsequent contractions at the warmer temperatures. In contrast, cooler muscles, with their reduced contraction rates, contracted with unfused tetany (Fig. 2.4A). Once again, we saw no statistical difference in the response to temperature between $DLM_{1c–e}$ and $DLM_{1a,b}$ (ANOVA, $P>0.15$; Table 1) other than at 40ºC (ANOVA, $P<0.05$). Change in temperature had a significant effect on the timing of peak force in all DLM_1 groups tested (ANOVA, $P<0.0001$). All pairwise comparisons show that the time of peak force occurred significantly earlier in the contraction cycle with each increase in temperature (Tukey–Kramer HSD, $P<0.05$; Fig. 2.4B). From 25 to 35ºC peak force of $DLM_{1c–e}$ and $DLM_{1a,b}$ combined occurred 37.4% earlier in the contraction cycle.

2.4.3 Extracellular evoked potentials

To determine whether the muscle subunits are activated simultaneously regardless of local temperature, we compared EMGs of the two most extreme subunits, DLM_{1a} and DLM_{1e} (Fig. 2.5). The timing of extracellular evoked potentials between these two subunits was statistically different for each individual (*t*-test, $P<0.01$). However, the mean difference in timing across all individuals was only 0.22±0.12 ms. This difference is a mere 0.6% of the characteristic 40 ms wingbeat cycle. The mean temperature difference between DLM_{1a} and

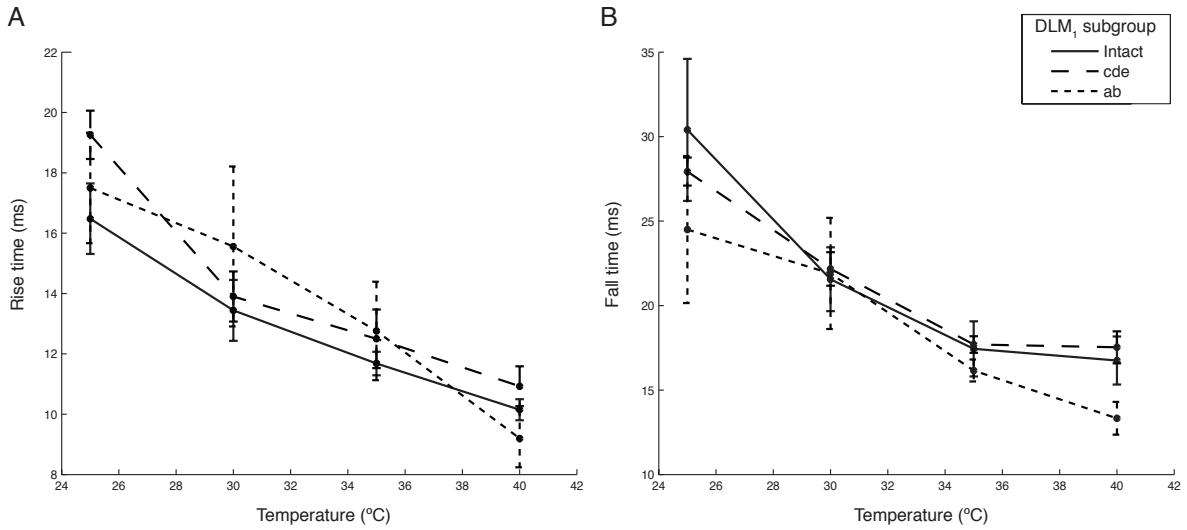

Figure 2.3: Mean rise times (A) and fall times (B) of single isometric twitches are plotted as a function of temperature. The rise and fall times of a contraction were calculated as the time at which the instantaneous force was 10% of the peak force. We found no statistical difference in the rise and fall times between $DLM_{1c–e}$ and $DLM_{1a,b}$ from 25 to 35ºC (ANOVA, $P>0.1$; Table 1), but the contraction dynamics of the three different groups (intact DLM_1, $DLM_{1c–e}$, $DLM_{1a,b}$) were significantly affected by the change in temperature (ANOVA, $P<0.05$). Values reported as means ± s.e.m (N=5 moths per group).

Table 2.1: ANOVA *P*-values for the mean rise time, fall time, and time of peak force of the more dorsal subunits ($DLM_{1c–e}$) compared with the ventral-most subunits ($DLM_{1a,b}$) of *Manduca sexta* flight muscle. N=5 moths per group. *, values are significantly different.

	ANOVA p-values		
Temp (ºC)	Rise times	Fall times	Time of peak force
25	0.3448	0.3668	0.2432
30	0.5617	0.9396	0.4513
35	0.9017	0.1144	0.3477
40	0.1698	0.0113*	0.0315*

Table 2.2: Mean rise and fall times recorded from single isometric contractions at different temperatures for three *M. sexta* muscle preparations: (1) intact DLM_1 comprised of all five subunits, (2) the dorsal-most subunits ($DLM_{1c–e}$) and (3) the ventral-most subunits ($DLM_{1a,b}$). Values reported as mean ± s.e.m. (N=5 moths per group).

	Rise time means (ms)			Fall time means (ms)		
Temp ºC	Intact DLM_1	DLM_{1cde}	DLM_{1ab}	Intact DLM_1	DLM_{1cde}	DLM_{1ab}
25	16.48±1.17	19.26±0.80	17.50±1.83	30.40±4.20	27.93±0.83	24.50±4.35
30	13.44±1.01	13.90±0.83	15.56±2.65	21.56±1.89	22.17±0.99	21.90±3.29
35	11.68±0.39	12.50±0.97	12.76±1.63	17.44±1.63	17.70±0.49	16.16±0.65
40	10.15±0.35	10.93±0.66	9.20±0.96	16.75±1.42	17.53±0.95	13.33±0.97

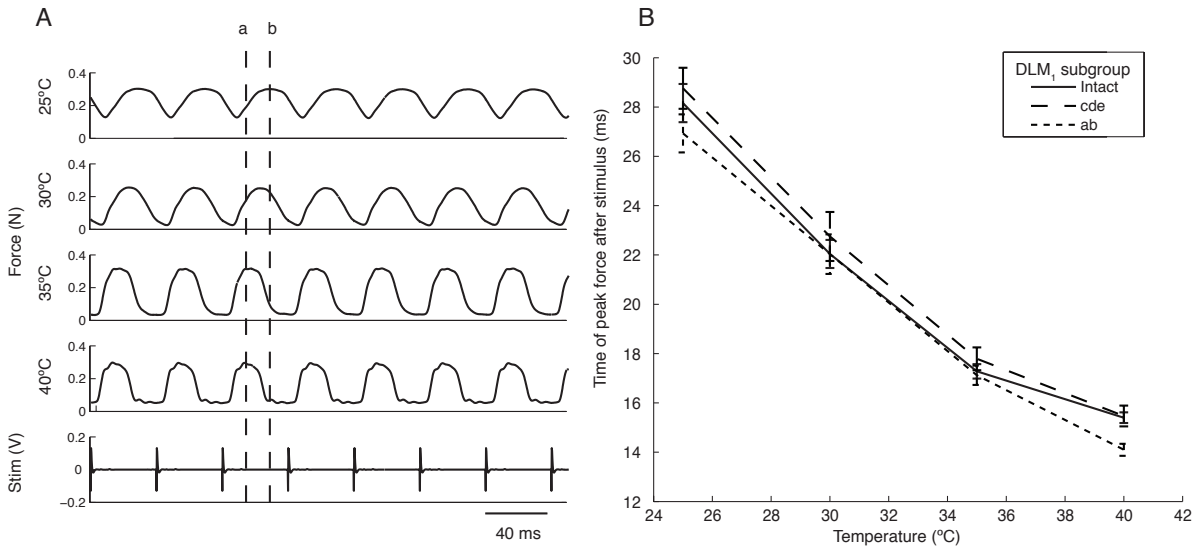

Figure 2.4: (A) Force plots of 25 Hz isometric contractions at 25, 30, 35, and 40ºC. The sequences shown are from an individual moth with intact DLM_1. At 40ºC the muscles fully relaxed before the next nerve impulse. As muscle temperature decreased, contraction rates also decreased. As a result, DLM_1 at 25ºC were unable to completely relax between contractions, resulting in unfused tetany. To determine how the different subunits respond to temperature at 25 Hz, we compared the time at which peak force occurred in relation to the contraction cycle (a, peak of 40ºC; b, peak of 25ºC). (B) In all three DLM_1 groups, peak force occurred significantly later in the contraction cycle as muscle temperature decreased (ANOVA, $P<0.0001$; Tukey–Kramer HSD, $P<0.05$). There was no statistical difference between the three groups from 25 to 35ºC (ANOVA, $P>0.15$; Table 1). Values reported as means ± s.e.m. (N=5 moths per group).

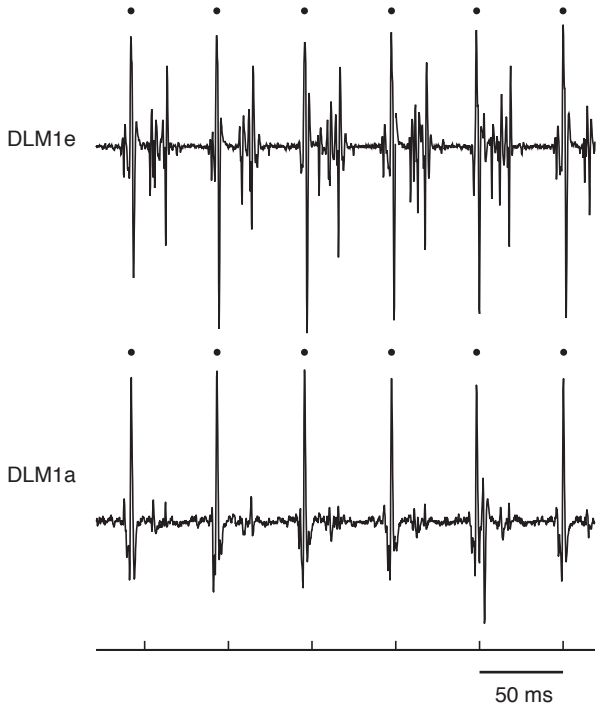

Figure 2.5: Two simultaneously recorded EMG sequences from DLM_{1e} (dorsal-most subunit) and DLM_{1a} (ventral-most subunit). The extracellular evoked potentials were recorded with two differential electrodes placed in the moth's thorax during tethered flight. There was a statistically significant difference of 0.22±0.12 ms (s.e.m.) between these two most extreme subunits (*t*-test, $P<0.01$; N=10 moths).

DLM_{1e} for these trials (6.2±0.6ºC) was similar to the temperature difference in the temperature profile trials (5.6±0.3°C).

2.5 Discussion

Several important results emerge from our study on temperature gradients and their functional consequences. First, metabolic heat production paired with heat-loss mechanisms necessarily leads to a substantial temperature gradient in the flight muscles of *M. sexta*. Second, given our measurements of force and electrical activity, the DLM_1 do not appear to be regionally specialized. Third, contractile performance of the DLM_1 subunits showed a temperature-dependent response consistent with prior studies (Bennett, 1984; Johnson and Johnston, 1990; Rall and Woledge, 1990). Combined, these results indicate that a temperature gradient will yield a functional gradient in the time course of force output of flight muscle, suggesting that a mechanical energy gradient is a direct consequence of a thermal energy gradient. Below, we elaborate on the consequences of this temperature gradient and its implications in the production and storage of energy in the musculoskeletal system.

2.5.1 Significant in vivo temperature gradient

Results from our spatial and temporal temperature measurements during tethered flight show a strong temperature gradient in the dorso-ventral direction. Regardless of the amount of scales covering the thorax, we saw a mean temperature difference of ~6ºC across a mere 5 mm of muscle. This surprisingly large gradient across such a small spatial scale should occur in both tethered and free flight because metabolic heat production and convective and radiative heat loss are processes that would occur in both flight regimes. Convective heat loss in tethered and free-flying animals should be similar, as wing motions in tethered flight induce a significant local flow that is close to those associated with free flight (Sane and Jacobson, 2006). Moreover, because free-flight thoracic temperatures have been recorded at ~41ºC, compared to tethered flight temperatures at 30–35ºC, we might expect an even larger, more functionally significant gradient to occur in natural flight (Heinrich, 1971). Thus,

temperature gradients throughout the dominant flight muscles may be a common occurrence for a wide range of large insects able to elevate their core temperature, spanning numerous orders (e.g. Lepidoptera, Orthoptera, Hymenoptera, and Coleoptera). Indeed, as we discuss below, temperature gradients in muscle may be more ubiquitous than previously thought.

2.5.2 No detectable regional specialization in contractile dynamics and neural activation

We found no evidence that the DLM_1 subunits employ varying regional twitch characteristics. Our isometric contraction tests did not reveal any significant difference between the outermost DLM_1 in their temperature dependence of twitch timing and contraction dynamics. The temperature dependence we observed was comparable to that in previous studies; both the rise time and fall time decreased as temperature was increased (Bennett, 1984; Josephson, 1984; Rall and Woledge, 1990; Marden, 1995). The rise and fall times of the intact DLM_1 group had Q_{10} values of 1.41 and 1.74, respectively, across a temperature range of 25–35ºC (Bennett, 1984). It is also important to note that although the greatest temperature difference of ~6ºC occurred between DLM_{1a} and DLM_{1e}, there was still around a ~4ºC difference between DLM_{1a} and DLM_{1d}. Though our studies did not show statistical differences for trials separated by 5ºC, Josephson (Josephson, 1984) found that the rise time and fall times of the mesothoracic first tergocoxal muscle of *Neoconocephalus robustus* decreased by ~30% and 20%, respectively, from 25 to 30ºC. In addition, our data show that the mean time of peak force for contractions at 25 Hz occurred ~21% earlier in the cycle when temperature increased from 25 to 30ºC. This indicates that temperature differences of ~5ºC could have significant functional consequences. Combined with our observation of decreasing temperature associated with progressively more fused contractions at 25 Hz, it is likely that the cooler muscles undergo reduced cross-bridge cycling and thus have diminished mechanical work output. At the highest temperature, 40ºC, we did observe a modest difference between the ventral and dorsal subunits; however, these subunit differences were much smaller than the effect of varying temperature regimes (Fig. 2.3 and 2.4B). In addition, our measurement of separate DLM_1 subunit evoked potentials showed only a minor difference, 0.22 ms, in activation times. Although this difference was statistically different from zero, the greater delays in the time of peak force during 25 Hz

contractions associated with decreased temperatures indicate that it will not result in a functional difference (Fig. 2.4).

Given the constraints of our experimental preparation, isolation and stimulation of individual muscle subunits was not easily achieved. Instead we chose to resolve the regional twitch dynamics at the spatial scale of 2-3 subunits. It is possible that individual subunit differences could be masked by more dominant muscles. However, given our data, we can claim that the more dorsal DLM_1 and the more ventral DLM_1, which have on average different operating temperatures, exhibit similar temperature-dependent responses in terms of contractile dynamics.

2.5.3 Temperature gradients induce mechanical gradients

Because there was no significant difference in twitch timing between muscle subunits, any spatial variation in contractile dynamics will largely be a consequence of spatial variation in temperature. Decreased contraction rates and unfused tetany at cooler temperatures suggests that dorsal subunits will undergo a substantially smaller length change than the warmer, ventral subunits. Therefore, the dorsal-most subunits of the DLM_1 may produce significantly less mechanical power, and thus could serve a primary function other than that associated with direct wing movement. Interestingly, a previous study has shown body temperature in *M. sexta* must be ~32ºC for take-off and ~29ºC for horizontal flight (McCrea and Heath, 1971). This observation is consistent with our findings that unfused tetany occurred at temperatures ~25ºC, indicating that there may be insufficient power output at these temperatures for the required locomotor performance. Stevenson and Josephson have already demonstrated a strong relationship between muscle temperature and power output in *M. sexta* (Stevenson and Josephson, 1990): from 40 to 20ºC, mean maximal power output decreased by ~70 W kg^{-1}. In that study, an optimal phase of activation was used to produce maximal power output; therefore, all temperatures led to positive power output. However, Tu and Daniel found surprisingly few phases of activation generate positive mechanical power output, with the *in vivo* phase and length change generating only 40-67% of the maximal realizable power output (Tu & Daniel, 2004b). Therefore, it is highly possible that cooler, dorsal subunits may produce close to zero or negative power output.

The functional consequences of a temperature-induced mechanical energy gradient could have significant effects on locomotor performance. Because temperature modulates function, a temperature gradient suggests that the DLM_1 may have multiple functions. The consequences of such regional functional specialization for power output in the DLM_1 are not yet known. We suggest that while ventral subunits are the main power generators, depressing the wings, more dorsal subunits exhibit progressively reduced power output following the decrease in temperature. Thus, cooler subunits could operate with: (1) a reduced but still positive power output; (2) near zero power output, allowing them to behave as springs; or (3) negative power output, thereby acting as dampers on the system. The notion that dorsal subunits could behave as springs that, at the end of the contraction, act in concert with the dorsoventral muscles to elevate the wings is consistent with a prior study on asynchronous muscles (Dickinson et al., 2005). Thus, although it is generally presumed that the rubber-like protein within the cuticle, resilin, is the main site of energy storage for insect flight (Gosline et al., 2002), recent research on asynchronous muscle in *Drosophila* suggests a significant amount of energy storage resides in the myofilaments and cross-bridges themselves (Dickinson and Lighton, 1995; Dickinson et al., 2005). Cooler, dorsal subunits operating with zero power output suggests yet another method by which energy production and storage could be regulated. The dorsal DLM_1 may serve as an elastic restoring force on the cuticle, with cross-bridges remaining, on average, more attached to the thin filaments and potentially serving a spring-like function. Potential mechanical energy stored in the cross-bridges from elastic deformation could be released as kinetic energy during the second phase of the wingbeat cycle. Thus, the cooler subunits would reduce the work required to elevate the wings and enhance the efficiency of flight. The extent to which the power output profile advantageously benefits from the induced temperature gradient warrants further examination. Ultimately, these temperature-induced functional differences propose a flight system that is capable of adjusting the energetic input and output on multiple levels.

Importantly, since muscles generate heat and experience convective and radiative cooling at the surface, muscle temperature gradients in a wide range of moving animals may be more prevalent than previously assumed. Though there are surprisingly few instances documenting temperature gradients in the literature, temperature differences of 3-5ºC and 10ºC have been reported in mammalian quadricep muscles (Jones et al., 2004) and

throughout the body of big-eye tuna (Carey and Teal, 1966), respectively. Although regional contractile performance was not evaluated in these cases, mammals and fish are known to experience increased contractile rates with increases in temperature (Carey and Teal, 1966). It is therefore reasonable to assume that a functional gradient could follow the temperature gradient in these organisms. Thus, the presence of an induced functional gradient could have profound implications to our understanding of energy storage and production in the musculoskeletal system.

2.6 List of symbols and abbreviations

DLM_1 dorsolongitudinal muscles
$DLM_{1a,b}$ ventral-most subunits
$DLM_{1c–e}$ dorsal-most subunits
EMG Electromyographic

2.7 Acknowledgements

We would like to thank Emily Carrington, Ray Huey, Simon Sponberg, Jessica Fox, Dave Williams, and Chet Moritz for their helpful insight. This research was supported by an NSF Graduate Research Fellowship to N.T.G., NSF Grant (IOS-1022471) to T.L.D. and the University of Washington Komen Endowed Chair to T.L.D.

Chapter 3

TEMPERATURE GRADIENTS DRIVE MECHANICAL ENERGY GRADIENTS IN THE FLIGHT MUSCLE OF *MANDUCA SEXTA*

Nicole T. George, Simon S. Sponberg, and Thomas L. Daniel

J Exp Biol, 2012

DOI: 10.1242/jeb.062901

3.1 Abstract

A temperature gradient throughout the dominant flight muscle (dorsolongitudinal muscle, DLM_1) of the hawkmoth *Manduca sexta*, together with temperature-dependent muscle contractile rates, demonstrates significant spatial variation in power production is possible within a single muscle. Using *in situ* work-loop analyses under varying muscle temperatures and phases of activation, we show that regional differences in muscle temperature will induce a spatial gradient in the mechanical power output throughout the DLM_1. Indeed, we note that this power gradient spans from positive to negative values across the predicted temperature range. Warm ventral subunits produce positive power at their *in vivo* operating temperatures, and therefore act as motors. Concurrently, as muscle temperature decreases dorsally, the subunits produce approximately zero mechanical power output, acting as an elastic energy

storage source, and negative power output, behaving as a damper. Adjusting the phase of activation further influences the temperature sensitivity of power output, significantly affecting the mechanical power output gradient that is expressed. Additionally, the separate subregions of the DLM_1 did not appear to employ significant physiological compensation for the temperature-induced differences in power output. Thus, although the components of a muscle are commonly thought to operate uniformly, a significant within-muscle temperature gradient has the potential to induce a mechanical power gradient, whereby subunits within a muscle operate with separate and distinct functional roles.

3.2 Introduction

Metabolic heat production, a byproduct of muscle contraction, can lead to a core body temperature that is significantly higher than ambient temperature. Many organisms from large insects to mammals benefit from the enhanced muscle performance that arises from this elevated temperature. Specifically, the rates of force production and the magnitude of power produced by muscle significantly increase with an increase in temperature (Bennett, 1984, 1985; Josephson, 1984; Rall and Woledge, 1990; Stevenson and Josephson, 1990; Swoap et al., 1993; Rome et al., 1999;). Therefore, temperature-dependent changes in muscle activity can have important functional consequences for the performance of animal locomotion. Yet the temperature of an animal's musculature does not necessarily need to be spatially uniform. Metabolic heat production paired with convective and radiative cooling to the surrounding environment can potentially create a temperature gradient even in a single muscle. For example, we previously showed that a significant dorso-ventral temperature gradient arises during tethered flight, with a temperature difference of ~6ºC, throughout the dominant flight muscle of the hawkmoth *Manduca sexta* (George and Daniel, 2011). Because muscle contractile rates and power production are temperature-dependent, functional heterogeneity may therefore occur within a single muscle. Thus, although it is clear that *in vivo* temperatures affect muscle function, the question remains, can an *in vivo* temperature gradient actually produce a mechanical and functional gradient that is not apparent if we consider the whole animal to operate at one uniform temperature?

Work-loop studies, where muscle is cyclically oscillated and periodically stimulated,

provide a means to determine how various neural and mechanical determinants, including muscle strain, length, and phase of activation (the timing of muscle stimulus relative to the strain cycle), influence mechanical power output across a range of operating conditions (George and Daniel, 2011). Although these work-loop studies have elucidated how muscle mechanics affect animal locomotor performance, they have generally assumed that a given muscle has a spatially uniform temperature and thus generates a spatially uniform function under a given set of conditions. Despite growing evidence showing that functional heterogeneity may occur within regions of a muscle because of morphological or neurological differences [e.g., fiber type (Mu and Sanders, 2001; Wang and Kernell, 2001), segment strain (Ahn and Full, 2002; Pappas et al., 2002; Higham et al., 2008; Higham and Biewener, 2008), motor recruitment (English et al., 1993; Holtermann et al., 2005; Wakeling, 2009), and neural activation (Sponberg et al., 2011)], the role of the physiological environment in which the muscle operates has generally not been considered. Given the notable Q_{10} of the physiological properties of muscle and the presence of thermal gradients, temperature itself likely produces significant functional differences within a single muscle. Thus, although muscles are classically thought to function solely as a motor, spring, brake, or strut, in some cases they may actually concurrently operate with an array of functions as a consequence of an internal temperature gradient (Altringham et al., 1993; Full et al., 1998; Dickinson et al., 2000). Using work-loop techniques conducted at different temperatures, we can examine how muscles respond to temperature gradients under *in vivo* stimulus and strain conditions.

The dorsolongitudinal muscle (DLM_1) (*sensu* (Kondoh and Obara, 1982), which is the dominant downstroke flight muscle of *M. sexta*, is an excellent system for a study of the functional consequences of a within-muscle temperature gradient. The DLM_1 consists of 5 separate muscle subunits – $DLM_{1a–e}$ – that are each approximately 1 mm thick (Fig. 3.1) (Eaton, 1988). Each of these separate subunits is innervated by a single motor neuron, four originating from the pterothoracic ganglion, while the fifth resides in the prothoracic ganglion with a long projection to DLM_{1e} (Kondoh and Obara, 1982; Eaton, 1988). Despite this potential for separate modulation, previous recordings indicate that all five separate subunits are activated nearly simultaneously by their respective motor neurons (George and

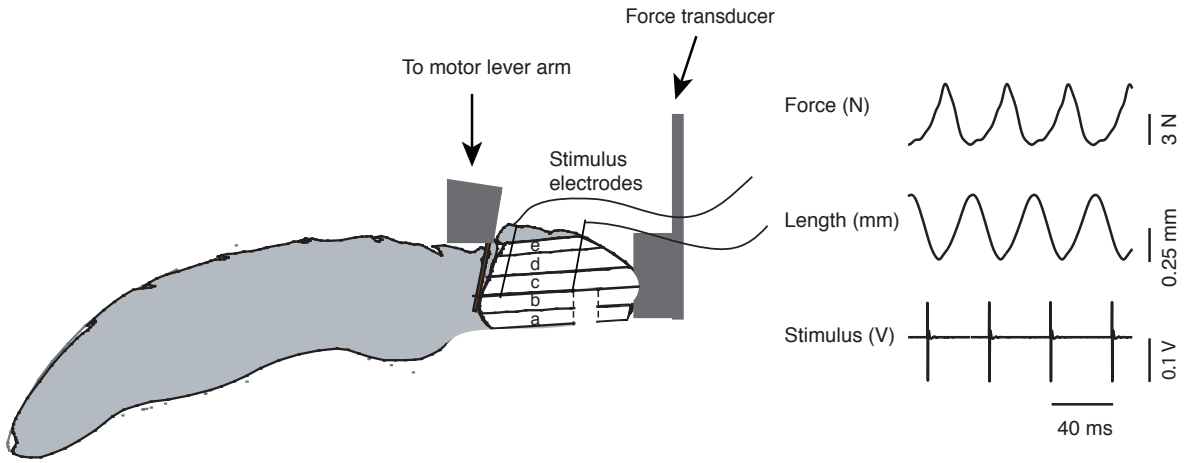

Figure 3.1: *Manduca sexta* preparation (head, wings, legs and scales removed) for the work-loop studies and an example trace of the force, length, and stimulus pattern. The thorax of *M. sexta* was fixed between an anterior grip attached to a force transducer and a posterior grip attached to a motor lever arm. A circumferential strip of cuticle ~2mm wide was excised from the middle of the thorax. The dorsoventral muscles and leg muscles were then removed to isolate just the dorsolongitudinal muscle (DLM_1) between the motor and force transducer. The DLM_1 was cyclically oscillated at 25 Hz by the motor lever arm with a strain amplitude of ~0.5 mm. At specific phases of each length cycle, the muscle wsd stimulated with 0.2 ms supramaximal stimuli. The force transducer then detected force output by the DLM_1. For these experiments, the DLM_1 subunits were either left intact or the dorsal (DLM_{1D}; depicted here) or ventral (DLM_{1V}) subunits were isolated. Figure adapted from Tu and Daniel (Eaton, 1988).

Daniel, 2011). Furthermore, these muscle subunits each fire with a one-to-one relationship with the motor neurons: each action potential elicits only one muscle contraction (Kammer, 1968).

Because of these properties, the DLM_1 is commonly thought to operate uniformly as a power generator to indirectly depress the wings. However, *M. sexta*'s highly elevated core temperature during flight (~40–43ºC maximum, ~15–25°C above ambient temperature) indicates that a significant temperature and functional gradient will exist throughout the flight musculature (McCrea and Heath, 1971; Heinrich and Casey, 1972). Although no attempt has yet been made to record a temperature gradient during free flight, the increased mechanical demands of free flight should lead to a temperature difference even greater than the ~6ºC difference recorded during tethered flight (George and Daniel, 2011). The most ventral DLM_1 subunit likely operates near the maximum-recorded temperature (~40ºC). Muscle temperature would then progressively decrease in the dorsal direction because of convective heat loss, with the superficial, dorsal-most subunit operating only slightly above ambient temperature (~25–30ºC). Because the rate of muscle force generation depends strongly on temperature, this regional difference in temperature might induce significant mechanical differences across the muscle.

A potential gradient in mechanical power output would have important implications for the production, storage, dissipation, and transmission of energy through the musculoskeletal system. Indeed, the warmer ventral subunits may act more as force generators, whereas the cooler dorsal subunits could act as springs, or even as damping elements. To test whether the power–temperature relationship of the DLM_1 would lead to regionally distinct functional roles, we conducted *in situ* work-loop studies on the DLM_1 at the *in vivo* phase of activation while varying muscle temperature from 25 to 40ºC.

Regional specialization of the contractile machinery could compensate for the thermal gradients, providing a spatially uniform level of power output. Thus, we performed the same mechanical tests on isolated dorsal or ventral subunits of the DLM_1. If compensatory mechanisms maintain a uniform function across the DLM_1, then power output of dorsal versus ventral subunits would be comparable when each is operating at its respective *in vivo* temperatures (~25–30ºC for dorsal subunits versus ~35–40ºC for ventral subunits).

Lastly, it is a common property of muscle that altering the time at which activation

occurs in relation to the strain cycle can lead to significant differences in power output (Josephson, 1985; Stevenson and Josephson, 1990; Tu and Daniel, 2004b). Recent evidence demonstrates that moths use neural feedback to actively modulate this phase of muscle activation during turning maneuvers (S. Sponberg and T. L. Daniel, unpublished). Therefore, in order to consider the role functional heterogeneity could play in controlling movement, it is important to examine how the phase of activation may alter the temperature sensitivity of mechanical power output. To test whether the power–temperature relationship itself depends on the phase of activation, we conducted additional temperature-controlled work-loops while varying the timing of muscle activation.

3.3 Materials and methods

3.3.1 Moths

Manduca sexta (L.) were obtained from a colony maintained by the Department of Biology at the University of Washington, Seattle, WA, USA. After eclosion moths were kept in 24 hrs of light. Moths were used within 5 days of eclosion.

3.3.2 Experimental apparatus and muscle preparation

Work-loop methods were adapted from Tu and Daniel (2004b) and George and Daniel (2011). Moths were held at ~4ºC for at least half an hour and up to one day prior to each experiment to immobilize them for experimental preparation. We first weighed each moth and measured the resting length of its mesothorax with digital calipers. The head, prothorax, wings, legs, and scales covering the thorax were then removed.

We conducted our work-loops using a semi-intact preparation, with the abdomen and tracheae undamaged. This allowed the DLM_1 to continue receiving a supply of oxygen and to remain viable throughout experiments. The DLM_1 was isolated between two grips; an anterior grip attached to a force transducer (Fort100, WPI, Sarasota, FL, USA) and a posterior grip mounted on a length driver (Model 305B Dual-Mode Lever Arm System, Aurora Scientific Inc., Aurora, ON, Canada) (Fig. 3.1). The length driver was tuned for the

added mass of the grip plus the moth body until the system produced smooth length control. The anterior grip, a small brass block shaped to fit the anterior mesoscutum and first phragma, was secured to the mesothoracic cuticle with a mixture of cyanoacrylate and sodium bicarbonate powder. To facilitate adhesion, the dorsal aspect of the anterior half of the mesothoracic cuticle was first lightly scored. The posterior grip, consisting of two stainless steel needles (15 mm long, diameter of 0.68 mm) soldered to a small brass block, was inserted along the posterior face of the mesothorax and secured with a drop of cyanoacrylate. A strip of cuticle, ~2 mm wide, was then excised from around the mid mesothoracic region. In addition, the antagonistic dorsoventral muscles along with the ventral aspect of the mesothorax just below DLM_{1a} were removed. This assured us that just the DLM_1 was mechanically isolated between the motor lever arm and force transducer. The force transducer was mounted to a micromanipulator, allowing us to adjust the length of the DLM_1 to the operating thorax length (0.98±0.02 of the rest length) (Tu and Daniel 2004a). Two tungsten electrodes (~10 mm long), inserted through the posterior and anterior notum along the same longitudinal transect of the DLM_1, connected to a stimulator (PG4000 Digital Stimulator, Neuro Data Instruments Corp, East Stroudsburg, PA, USA) delivered 0.2 ms supramaximal stimuli (~600–900 mV) at 25 Hz (normal wingbeat frequency), consistent with prior studies (Tu and Daniel, 2004b; George and Daniel, 2011). Evoked potentials were recorded with a bipolar differential tungsten electrode inserted near the posterior grip and a common reference wire placed in the abdomen. The signal was amplified (x1000) with a differential AC amplifier (model 1800, A-M Systems, Sequim, WA, USA) and band pass filtered (300-20 kHz).

Immediately after each experiment, the moth's thorax was carefully removed from the grips and placed in *M. sexta* saline (Lei et al., 2004). We then removed the remaining DLM_1 from the mesothorax. The DLM_1 was quickly blotted with a tissue and weighed to the nearest 0.1 mg.

Work-loops were conducted on three separate muscle preparations to test for possible regional differences in the power output sensitivity to temperature: (1) DLM_1 with all 5 subunits intact (intact DLM_1), (2) DLM_1 with the ventral subunits cut through, leaving just the dorsal subunits intact (DLM_{1D}; Fig. 3.1), and (3) DLM_1 with the dorsal subunits cut, leaving the ventral subunits intact (DLM_{1V}) (N=5 moths per subgroup). Given the constraints

of muscle isolation and stimulation, we were unable to compare the power output of individual DLM_1 subunits. Instead, we were confined to resolve power output at the spatial scale of two to three subunits. However, the mean *in vivo* operating temperatures of the dorsal and ventral subunits would still be significantly different. Thus, comparing power output in response to temperature at this spatial scale would be sufficient to determine whether compensatory mechanisms exist.

To minimize the experiment duration and to preserve muscle tissue, we heated the DLM_1 sequentially rather than randomly. To determine whether the muscle significantly fatigued during the ~20 min test period, we did an additional set of 'control' work-loop tests in which we repeated the previous stimulation procedure and experiment duration but held the muscle temperature at 35ºC (*N*=5 moths).

3.3.3 Muscle length and strain

The DLM_1 was electrically stimulated and sinusoidally lengthened for 2 s, with a peak-to-peak strain amplitude of ~0.5 mm (~±2.5% of the initial muscle length), a duty factor (calculated as the fraction of time spent shortening during the length cycle) of ~0.5, and a frequency of 25 Hz (see Tu and Daniel, 2004a). The DLM_1 undergoes a net shortening during flight; the mean *in vivo* operating length is 0.98±0.02 of the rest length (Tu and Daniel, 2004a). We measured the rest length of the thorax while the moth was immobilized from cold exposure, and then set the starting experimental length of the DLM_1 to the calculated operating length.

The limitations inherent with conducting *in situ* work-loops on *M. sexta* required that the actual length changes we were able to impose differed from the *in vivo* strain. The large inertial mass of the *M. sexta's* body oscillating on the motor lever arm limited us to induce strains that were only a fraction (~50%) of *in vivo* strain (Tu and Daniel, 2004a). The slight intra–animal variability in strain trajectory may have been because of unavoidable differences in body size, motor unit recruitment, and the magnitude of muscle force output. Despite these complications with imposed strain, Tu and Daniel (2004b) found that the effect of strain amplitude on the magnitude of power output of the DLM_1 was relatively small and did not influence the shape of the power-phase curve. In addition, we found that the effect of

temperature, phase and subunit was consistent across animals. Thus, we are confident that our data accurately reflect the mechanical and functional consequences of the temperature gradient.

3.3.4 Muscle temperature

To control muscle operating temperature, *M. sexta* saline in a flask seated on a heating apparatus was slowly dripped over the exposed DLM_1. The saline was gradually heated to elevate muscle temperature to 25, 30, 35, and 40ºC. We chose these values to encompass the full range of the possible temperature gradient during flight; from the mean temperature of the dorsal-most subunit recorded during tethered flight (~25ºC) to the maximum temperature recorded during free flight (~40ºC) (Heinrich and Casey, 1972; George and Daniel, 2011). Muscle temperature was measured with a thermocouple embedded in a 30 gauge hypodermic probe (HYP-1, Omega Engineering Inc., Stamford, CT, USA). Experiments were performed once the muscle thermocouple settled on the target temperature. This method was sufficient to control muscle temperature to within 1ºC over the course of each experimental trial.

3.3.5 Phase of activation

To test whether the power–temperature relationship for the DLM_1 or the subunits depended on the phase of activation, we repeated the 2 s series of work-loops, where the muscle was subject to controlled cyclic length changes, while monitoring force. We used four different phases of activation, ~0.18, 0.28, 0.46 (approximately *in vivo*), and 0.58, at each temperature while performing these work-loops (Tu and Daniel, 2004a). These phases were chosen to encompass a range surrounding the phase that produced peak positive power output (~0.36) as determined by Tu and Daniel (2004b). Here phase of activation is calculated as the duration of time from the start of muscle lengthening to the peak of the evoked action potential divided by the cycle period.

3.3.6 Data acquisition

Force, muscle length, and evoked potentials were recorded at 5000 Hz by a data acquisition

system (NI USB-6229, National Instruments, Austin, TX, USA). Evoked potentials were analyzed using custom-designed peak detection software in MATLAB (The MathWorks, Natick, MA, USA) developed by M. S. Tu (University of Washington, Seattle, WA, USA).

Net work per cycle was calculated by integrating force output with respect to muscle length. We calculated the net work for 20 cycles per trial, starting with the tenth cycle. Mass specific power output is the product of mean net work and cycle frequency (25 Hz) divided by the mass of the DLM_1.

3.3.7 Statistical analysis

Given the length of the experimental trials, different sets of 5 animals were used for the intact DLM_1 and for each of the two subgroup conditions. The experimental design was balanced for each of these trials. Results and statistical tests for each experimental condition are reported as means across individuals. A one-way ANOVA was employed to determine how power output depends on both temperature and phase of activation and whether these dependencies differ among subunit groups. A Tukey–Kramer honestly significant difference (HSD) test was then used to isolate specific differences between the means at each temperature and phase of activation. Non-parametric Wilcoxon tests gave similar results. Data are represented as means ± s.e.m. unless otherwise noted.

3.4 Results

3.4.1 Operating conditions

Mean body mass of the 15 moths used in these work-loop trials was 2.59±0.25 g (s.d.). Mean rest length of the mesothorax was 10.19±0.39 mm (s.d.). Mean thorax operating length was 9.91±2.74 mm (s.d.). Neither moth size nor mass differed significantly among the three groups tested (ANOVA, $P>0.1$). The mean peak-to-peak strain amplitude imposed on the DLM_1 was 0.48±0.04 mm (s.d.). This strain amplitude did vary slightly (~8%) between individuals because of the constraints of our *in situ* preparation, including the large mass of *M. sexta* on the motor lever arm, slight flexibility of the force transducer, and individual

variation in activation dynamics. The four phases of activation used in these preparations had mean values of 0.18±0.01, 0.28±0.02, 0.46±0.01, and 0.58±0.01 (s.d.). Mean muscle mass of intact DLM_1, DLM_{1D}, and DLM_{1V} after being dissected out of the thorax was 0.193±0.010, 0.169±0.023, and 0.112±0.019 g (s.d.), respectively. Mean muscle mass of the two isolated subunit groups sum to a value greater than the mean muscle mass of intact DLM_1 because we were not able to isolate DLM_{1D} and DLM_{1V} precisely at the subunit level while the animal was mounted in the work-loop apparatus (portions of the middle subunit were occasionally included in both groups).

3.4.2 Effect of temperature on power output at the in vivo phase of activation

We analyzed power output and its temperature dependence in intact DLM_1 at the *in vivo* phase of activation (~0.46) (Tu and Daniel, 2004a). Muscles were cyclically lengthened and stimulated at muscle temperatures of 25, 30, 35, and 40ºC. The mean value for power output of intact DLM_1 (~60 W kg^{-1}) at the *in vivo* phase of activation at 35ºC is consistent with the power output measured in a prior work-loop study on *M. sexta* (Tu and Daniel, 2004b).

We observed a strong temperature dependence of net work. The DLM_1 produced negative, approximately zero, and positive work-loops across the range of temperatures we predict to simultaneously occur within this muscle during sustained flight (25–40ºC; George and Daniel, 2011) (Fig. 3.2). For all individuals tested, the power output of intact DLM_1 (at the approximate *in vivo* phase of activation) was greatest at either 35ºC or 40ºC, and significantly decreased as temperature decreased. There were statistically significant differences in power output between each separate temperature point, with the exception of one individual from 35 to 40ºC (Tukey–Kramer HSD, $P<0.0001$; $P\approx0.1$ for 35-40ºC). With each moth, power output transitioned from positive to negative between 35 and 30ºC (Fig. 3.3 and Table 3.1). Mean power output of intact DLM_1 decreased from 60.53±3.40 W kg^{-1} at 35ºC, to –74.66±4.41 W kg^{-1} at 30ºC. Assuming a linear relationship between these temperatures indicates that the transition temperature for positive to negative power output occurs at ~33ºC. Because power output at the lower temperatures was negative we cannot calculate the Q_{10} of power output for these trials.

Although the coefficient of variation across the 20 work-loop cycles recorded for

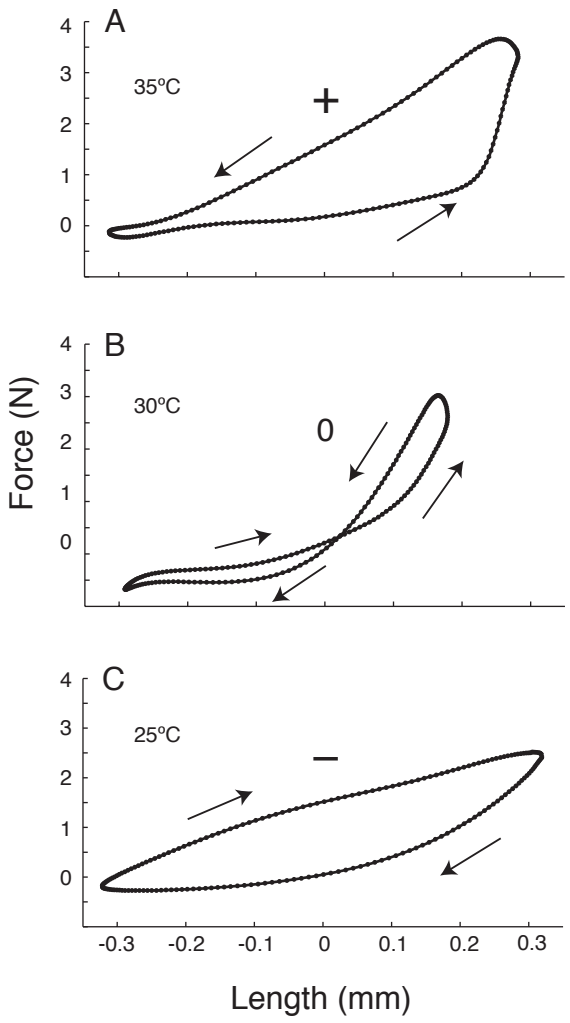

Figure 3.2: Example positive, approximately zero, and negative work-loops at (A) 35ºC, (B) 30ºC, and (C) 25 ºC. Net work is calculated as the area within each loop. The counterclockwise direction of work-loop A is indicative of positive work, or energy production. The clockwise direction of work-loop C is indicative of negative work, resulting in energy absorption. Net work became significantly more negative as temperature decreased. +, 0, or – signs indicate net energy generation, storage and return, or dissipation, respectively.

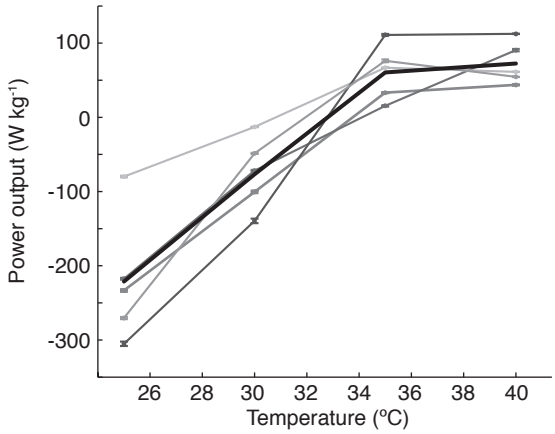

Figure 3.3: Temperature significantly affected power output in intact DLM_1. Mass specific power output is plotted as a function of temperature at the approximately *in vivo* phase of activation (0.46) for intact DLM_1. Each individual of the intact DLM_1 preparation is represented as a separate gray line. There were statistically significant differences in power output between each temperature point, except for one individual between 35-40ºC (Tukey–Kramer HSD, $P<0.0001$). The thick black line superimposed over the individual data represents the mean power output of all moths. Power output was positive between 40 and 35ºC and negative between 30 and 25ºC. Values are reported as means ± s.e.m. (N=5 moths, 20 cycles per trial).

Table 3.1: Mean power output for the *in vivo* phase of activation (0.46) at 25, 30, 35, and 40ºC for the three *M. sexta* preparations: (1) intact DLM_1 comprised of all five subunits, (2) the dorsal subunits (DLM_{1D}), and (3) the ventral subunits (DLM_{1V}).

	Power output (W kg $^{-1}$)		
Temp (ºC)	Intact DLM_1	DLM_{1D}	DLM_{1V}
25	–221.26±7.77	–125.80±4.62	–209.02±8.43
30	–74.66±4.41	–37.05±2.54	–63.72±2.98
35	60.53±3.40	32.42±3.29	26.72±1.62
40	72.50±2.57	62.14±4.99	87.50±2.75

N=5 moths per group, 20 cycles per trial. Values reported as means ± s.e.m.

each condition was small (0.18), there was significant variability in individual performance (ANOVA, F-ratio=36.4, P<0.0001; Fig. 3.3). However, the effect of temperature was greater than the effect of the individual on power output (mean difference of ~294 W kg^{-1} between 25 and 40ºC versus a mean maximum individual difference of ~129 W kg^{-1}; F-ratio ~29-fold greater for effect of temperature versus individual).

The results from our work-loop study were not confounded by a decline in performance during the experiment due to muscle fatigue. Routine muscle stimulation and contraction over a 20 min period in our fatigue controls did not produce significantly detectable changes in power output (a difference of ~5 W kg^{-1}, from 38.33±1.79 to 43.31±1.84 W kg^{-1}; ANOVA, P>0.1).

3.4.3 Subunit differences

Work-loops conducted on isolated dorsal (DLM_{1D}) and ventral (DLM_{1V}) subunits at the approximately *in vivo* phase of activation showed significant differences in power output between the two isolated subgroups, even when considering the effect of temperature (ANOVA, P<0.0001). In addition, the relationship between power output and temperature differed for DLM_{1D} and DLM_{1V} (ANOVA temperature–subgroup interaction, F-ratio=54.5, P<0.0001). Compared with the ventral subunit group, DLM_{1D} had a shallower mean power–temperature curve, with higher power output at 25ºC and lower power output at 40ºC (Fig. 3.4A, B). However, regardless of the increase in performance at cooler temperatures, DLM_{1D} would still fail to yield power output comparable to the ventral subunits at their warmer *in vivo* operating temperatures. At 30ºC, DLM_{1D} produced approximately –37 W kg^{-1}, yielding ~27 W kg^{-1} more than DLM_{1V} at the same temperature. This increase in power output of the dorsal subunits could only account for 22–42% of the rise in power output afforded by even a 5–10ºC increase in ventral subunit temperature (~64–124 W kg^{-1} more; Table 3.1). Furthermore, temperature had a more dominant effect on power output than did subgroup (mean difference of 242 W kg^{-1} between 25 and 40ºC versus a mean difference of 35 W kg^{-1} between DLM_{1D} and DLM_{1V}; F-ratio ~22-fold greater for the effect of temperature versus subgroup).

The small mechanical power differences between the dorsal and ventral groups at a

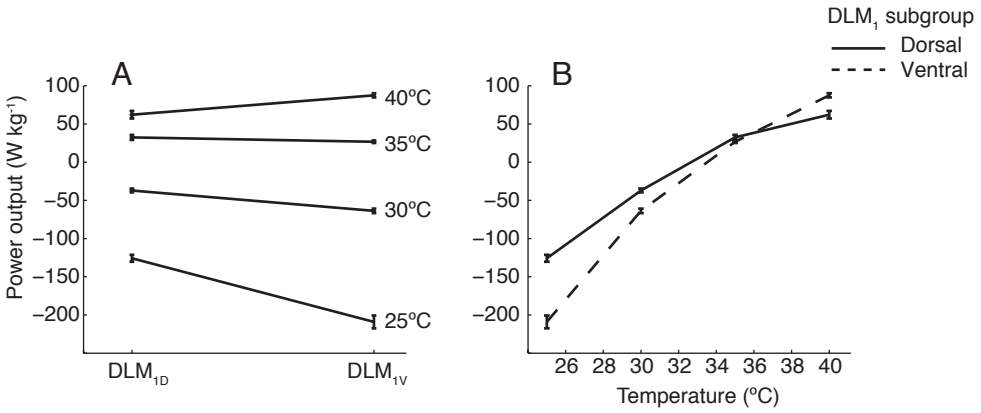

Figure 3.4: Mechanical power output of the dorsal subunits (DLM_{1D}) compared to the ventral subunits (DLM_{1V}) of *M. sexta* flight muscle at the approximately *in vivo* phase of activation. (A, B) Mean power output is plotted as a function of temperature for DLM_{1D} and DLM_{1V}. Although the two subunit groups had significantly different responses to temperature, this difference was not functionally significant. Mean power output for the two groups remained positive between 40 and 35ºC and negative between 30 and 25ºC. Values are reported as means ± s.e.m. (N=5 moths per group, 20 cycles per trial).

fixed temperature are overwhelmed by the very strong regional temperature-dependent power differences. DLM_{1D}, at the *in vivo* phase of activation and the predicted operating temperatures for the dorsal subunits (~25–30ºC), always produced net negative power. In contrast, DLM_{1V}, predicted to operate at the *in vivo* ventral subunit temperatures of ~35–40ºC, yielded positive mechanical power output. Thus, we do not find sufficient regional specialization in mechanical performance to negate the diversity in power output that will result from subunit specific *in vivo* operating temperatures.

3.4.4 Effect of phase of activation on the power–temperature relationship

Because of the temperature-induced gradient in the mechanical power output of the DLM_1, we investigated the potential for neural modulation to actively regulate the activity of the DLM_1. Work-loops of intact DLM_1 at four different phases of activation (0.18, 0.28, 0.46, and 0.58) show that phase and temperature interact to affect the mechanical power output of this muscle (Fig. 3.5A, B). For each phase of activation, a change in temperature from 25 to 40ºC significantly affected power output, with all but one pairwise increase in temperature being statistically different (ANOVA, $P<0.0001$; Tukey-Kramer HSD, $P<0.0001$). Interestingly, phase of activation also affected the actual relationship between power output and temperature (ANOVA temperature–phase interaction, F-ratio=219.8, $P<0.0001$). Early phases of activation (0.18 and 0.28) produced peak power at intermediate temperatures (30 or 35ºC), whereas later phases of activation (0.46 and 0.58) led to monotonically increasing power throughout the temperature range. As a consequence, maximum power output occurred at sequentially warmer temperatures as phase increased; for a phase of 0.18 mean maximum power output occurred at 30ºC, for a phase of 0.28 it occurred at 35ºC, and for phases of 0.46 and 0.58 it occurred at 40ºC (Fig. 3.5A and Table 3.2).

As mentioned above, the *in vivo* phase of activation (~0.46) yielded positive power only at 35 and 40ºC. Notably, advancing muscle activation to an earlier phase (e.g. 0.28) actually extended the temperature range across which positive power output was produced to 30–40ºC. Conversely, a later phase (e.g. 0.58) resulted in negative power output across all temperatures (Table 3.2). The *in vivo* phase was submaximal for power production at all temperatures, consistent with earlier single temperature results (Tu and Daniel, 2004b).

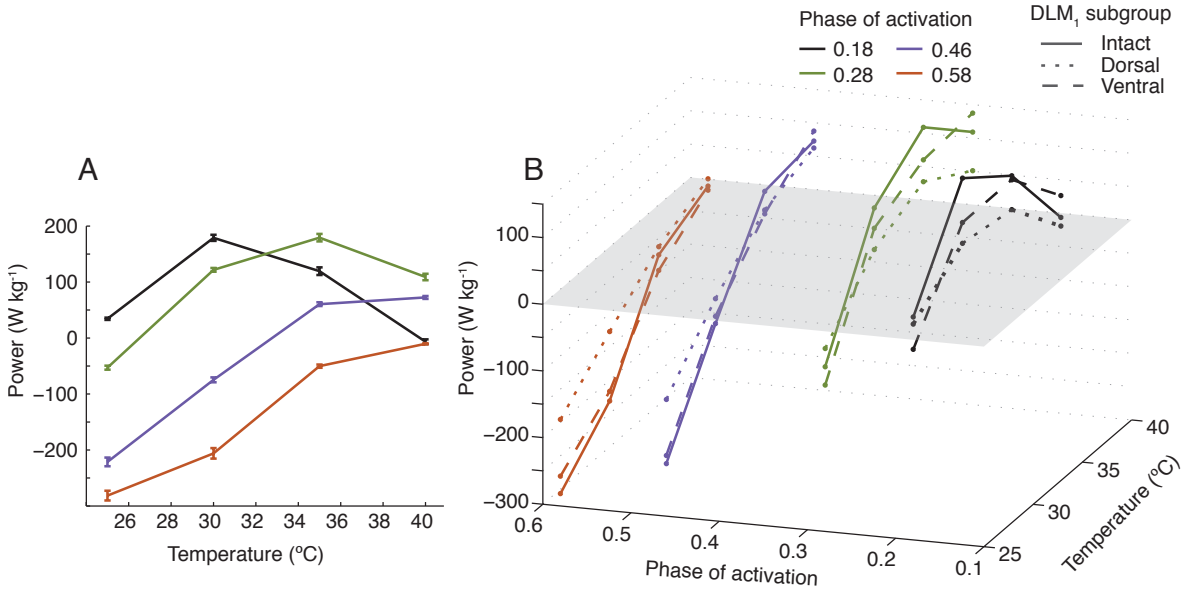

Figure 3.5: The effect of phase of activation on power output in the presence of a temperature gradient. (A) Mass specific power output for intact DLM_1 as a function of temperature for each phase of activation (0.18, 0.28, 0.46, and 0.58). Shifting the phase of activation results in a significantly different power-temperature relationship. Early phases of activation (0.18–0.28) produced peak power at intermediate temperatures (30 or 35ºC). Conversely, later phases of activation (0.46–0.58) resulted in monotonically increasing power output with temperature. (B) Mass specific power output as a function of temperature and the phase of activation. In the presence of a temperature gradient, adjusting the phase of activation represents a neuronal mechanism by which the organism could modify the functional gradient. The gray plane indicates the transition point between positive and negative power output. At approximately the *in vivo* phase, positive power was produced only between 40–35ºC. However, advancing the phase to ~0.28 increased the temperature range that produced positive power to 40–30ºC.Values reported as means ± s.e.m. (N=5 moths per group, 20 cycles per trial).

Table 3.2. Mean power output (W kg^{-1}) for intact DLM_1 across the temperature gradient for all phases of activation (0.18–0.58)

	Phase of activation			
Temp (ºC)	0.18	0.28	0.46	0.58
25	34.37±2.00	–52.93±3.57	–221.26±7.77	–281.43±8.67
30	179.02±5.46	121.76±3.36	–74.66±4.41	–206.04±9.41
35	119.40±6.77	179.28±6.71	60.53±3.40	–50.16±2.88
40	–6.59±4.17	109.01±5.70	72.50±2.57	–10.24±1.09

N=5 moths per group, 20 cycles per trial. Values reported as means ± s.e.m.

As with a phase of activation of 0.46, the two subunit groups, DLM_{1D} and DLM_{1V}, had different power–temperature relationships for the additional phases of 0.18, 0.28, and 0.58 (ANOVA temperature–subgroup interaction, F-ratio=21.5–81.6, P<0.0001) (Fig. 3.5B). Overall, at each phase of activation, DLM_{1D} and DLM_{1V} had power–temperature curves that were similar in shape to each other and to that of the intact DLM_1 group (i.e., either power monotonically increased with temperature or maximum power occurred at some intermediate temperature). However, at each phase, DLM_{1D} maintained a shallower power–temperature curve than DLM_{1V}, with comparatively higher power produced at cooler temperatures and lower power produced at warmer temperatures. Furthermore, the temperature point at which the power–temperature curves for DLM_{1D} and DLM_{1V} crossed was itself phase dependent. For early phases of activation (0.18–0.28), power output of DLM_{1D} and DLM_{1V} crossed between 25 and 30ºC, whereas for a phase of 0.46, power crossed at 35ºC, and for a phase of 0.58, based on the trajectories of the power–temperature curves, we predict power to cross at a temperature greater than 40ºC. However, the differences in power output between DLM_{1D} and DLM_{1V} were still relatively small compared to the effect of temperature (F-ratio ~5 to 8-fold greater for the effect of temperature *versus* subgroup). The difference in mean power output between the two subunit groups was never more than 40% of the total change in power caused by temperature. In addition, despite these differences in magnitude, the actual sign of power output, and therefore the functional role, did not change in either subunit group (with the exception of a phase of 0.18 at 25ºC, where power output only differed by ~37 W kg^{-1}).

3.5 Discussion

Our results show that a temperature gradient leads to a mechanical functional gradient within the DLM_1: as muscle temperature decreased from 40 to 25ºC, power output of the DLM_1 transitioned from positive values to considerably negative ones – leading to regions in which a single muscle may act more as an actuator, more spring-like, or more like a damping element. Although a small difference existed in the temperature-dependence of power output between the two subunit groups (DLM_{1D} and DLM_{1V}), these differences were not sufficient to account for the large variation in mechanical power output that resulted from the

temperature gradient predicted within the DLM_1 *in vivo* (10–15ºC). The combined evidence suggests that a functional gradient will follow the temperature gradient, with individual subunits of the DLM_1 contributing separately to energy production, storage, and/or absorption. In the discussion below, we expand upon our observations of a mechanical energy gradient and explore its implications for the coordinated muscle movement required for animal locomotion.

3.5.1 Temperature gradients within flight power muscles translate to functional gradients

Recent studies have revealed that muscles perform diverse functions to meet the fundamental demands of locomotion, including energy production, storage, absorption, and transmission (Lei et al., 2004). Thus muscles may act as actuators or may behave more like springs, struts, or even damping elements. However, these studies assumed spatially uniform temperatures within muscle, such that the contractile properties of the whole muscular unit follow from a spatially uniform mechanical behavior.

Temperature has a significant effect on muscle performance. Organisms across a range of habitats and locomotor modes experience increased contractile rates (i.e. activation and relaxation), and therefore increased mechanical power output, as muscle temperature increases (Josephson, 1984; Bennett 1985; Rall and Woledge, 1990; Swoap et al., 1993; Rome et al., 1999; Donley et al., 2007). For example, a 20ºC increase in muscle temperature yielded ~70 and 111 W kg^{-1} more specific mechanical power output in moths and lizards, respectively (Stevenson and Josephson, 1990; Swoap et al., 1993). Given this strong temperature dependence, the spatial pattern of temperature within a muscle may be a key factor determining overall muscle performance.

Our work-loop study revealed that power output of the DLM_1 was indeed highly temperature-dependent. Notably, across the temperature range that we expect to occur in the DLM_1 of *M. sexta* (~15ºC, from 40–25ºC), power output at the *in vivo* phase of activation transitioned from positive to highly negative values, with a mean difference of ~294 W kg^{-1}. Even a more conservative estimate of a temperature difference of 10ºC (from 40–30ºC) resulted in a shift from positive to negative power output with a mean difference of ~147 W kg^{-1} (Fig. 3.3; Table 3.1). Thus, without significant physiological differentiation among the

subunits of the DLM_1, ventral subunits will operate more as power producers while dorsal subunits, being significantly cooler, will operate as energy absorbers.

3.5.2 Differences in physiology across the muscle do not compensate for temperature gradients

Despite the presence of a temperature gradient, the DLM_1 could have a spatially uniform mechanical power output if appropriate physiological mechanisms could compensate for the local temperature. Spatially uniform power output throughout the DLM_1 could be accomplished by both extrinsic factors (i.e. neural activation) and intrinsic factors (i.e. fiber contractile dynamics).

Although each of the five DLM_1 subunits are separately innervated by neurons in the IIN_{1C} nerve (Kondoh and Obara, 1982; Eaton, 1988), allowing the potential for individual activation, they are effectively activated simultaneously (difference of only ~0.22 ms or ~0.6% of the wingbeat cycle; George and Daniel, 2011). Thus, moths do not appear to utilize dorso-ventral phase adjustments in muscle activation to yield increased power output in cooler dorsal subunits.

In addition, regional differences in the intrinsic properties of the muscle fibers comprising the DLM_1 could offset the consequences of temperature gradients. Prior studies have already demonstrated variation in both fiber type and contractile properties (i.e. activation and relaxation rates) across and within muscle (Swank et al., 1997; Mu and Sanders, 2001; Swank and Rome, 2001; Wang and Kernell, 2001), though not specifically within *M. sexta* flight muscle. Not surprisingly, varying the rate of muscle activation and relaxation greatly influences the magnitude of power produced in oscillatory movement (Rome and Swank, 1992; Josephson, 1993; Swoap et al., 1993; Swank and Rome, 2001). For example, a 20% decrease in twitch activation time associated with cold-acclimation resulted in up to a 2.5-fold increase in power production in fish muscle (Swank and Rome, 2001). Because of these observations, we must determine local responses to the temperature of subunits within a muscle before we can interpret the functional consequences of a temperature gradient.

Despite the small variation in the power–temperature relationship between ventral and dorsal DLM_1 subunits, this difference fails to be functionally significant. At the predicted

in vivo operating temperatures for the dorsal subunits, 25 and 30ºC, DLM_{1D} did produce higher power output than DLM_{1V}. However, this increase in performance was still significantly below the power produced by the ventral subunits at their predicted *in vivo* temperatures of 35 and 40ºC (Table 3.1). More importantly, the power produced by DLM_{1D} remained negative at 25 and 30ºC, whereas DLM_{1V} produced positive power at 35 and 40ºC. Thus, regional specialization of the DLM_1 subunits does not appear to compensate for the large temperature dependence in such a way as to produce uniform mechanical power output.

3.5.3 Implications for the role of different subunits in flight

Whereas the DLM_1 is generally assumed to solely produce power, driving the downstroke of the wing, we have demonstrated that muscle function in the DLM_1 may actually be systematically and heterogeneously distributed (Fig. 3.6). Warm ventral subunits, operating at ~35–40ºC, will produce positive power and drive wing depression. However, the dorsal subunits, operating at ~25–30ºC, will produce negative power and function more as energy absorbers, possibly contributing to the stability of the system. Interestingly, this transition in power output necessarily implies that at some midpoint in the DLM_1, muscle would generate little or no mechanical power; possibly providing a more spring-like behavior. This is not to say that the subunits could not all contribute to energy storage. Rather, we point out that a region of zero mechanical power output may still be functionally important.

Several studies suggest that elastic energy storage plays a crucial role in insect flight, allowing insects to reduce the inertial power costs of accelerating the wings (Alexander and Bennet-Clark, 1977; Ellington, 1985; Dickinson and Lighton, 1995; Wu and Sun, 2005). Although resilin, a rubber-like protein within cuticular structures, is presumed to be the main site of this energy storage (Jensen and Weis-Fogh, 1962; Haas et al., 2000; Gosline et al., 2002), a recent study found that thick filaments in asynchronous muscle deform elastically (Dickinson et al., 2005), indicating that a portion of energy storage could occur within the myofilaments themselves. We suggest that a temperature gradient, because of its effect on contraction dynamics within a single muscle, provides an additional mechanism for elastic energy storage to be utilized. The cross-bridges of the cooler dorsal subunits, with their

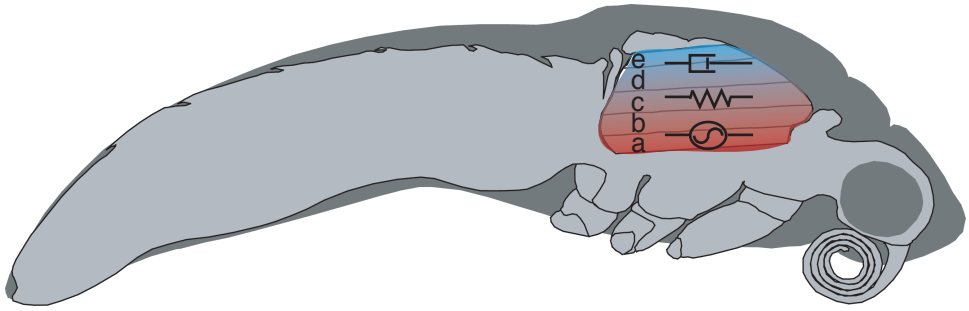

Figure 3.6: A schematic representation of a temperature-induced functional gradient. Proceeding from the ventral subunits to the dorsal subunits, the symbols represent a motor, a spring, and a dashpot. Our work-loop studies demonstrated that a temperature difference of 10–15ºC throughout the DLM_1 would lead to a significant gradient in mechanical power output. Warm ventral subunits operating around 40–35ºC would produce positive power and operate as a motor. Proceeding dorsally, mechanical power output of the DLM_1 subunits would decrease significantly with the decline in muscle temperature. Thus, more dorsal subunits, operating around 35–25ºC, would produce close to zero or negative mechanical power, and function more as an elastic energy storage source or more as a damper, respectively. Therefore, although the DLM_1 is commonly thought to function solely as a motor, a temperature gradient throughout the muscle will likely result in a spatial gradient of functional performance.

reduced cycling rates, would remain on average more attached to thin filaments, forming a locked spring lattice. Elastic energy could be stored in the cross-bridges and in the axial portions of the myofilament lattice as well. The stored mechanical energy could then be released during the next part of the wingbeat cycle, acting in concert with the antagonistic dorsoventral upstroke muscles to elevate the wings. Cross-bridges and the filament lattice could therefore contribute to the total energy storage needed for flight.

3.5.4 Implications for locomotor control

The timing of muscle activation relative to the length cycle significantly affects mechanical power output (Josephson 1985; Josephson, 1999; Tu and Daniel, 2004b). Several organisms use different phases of activation to enable functional diversity across different muscles (Tu and Dickinson, 1994; Altringham and Ellerby, 1999; Dickinson et al., 2000; Ahn and Full, 2002). In moths this dependence goes further, affording the organism a mechanism by which the nervous system can rapidly modulate muscle power output by adjusting the phase of the DLM_1 in response to sensory feedback from visual stimuli (S. Sponberg and T. L. Daniel, unpublished). Given this possibility of sensory feedback control, the phase of activation could additionally regulate the extent to which muscle function is diversified by influencing the relationship between power and temperature. During sustained flight, the DLM_1 of *M. sexta* activate just before shortening (phase of ~0.49) (Tu and Daniel, 2004a). At this approximate phase of activation, a 10ºC difference (40–30ºC) across the DLM_1 led to positive power output at 40 and 35ºC but negative power output at 30ºC. Delaying the phase to ~0.58 essentially led to negative power production at all temperatures. However, advancing the phase to ~0.28 actually increased the effective temperature range that yielded positive power output to 40–30ºC. Thus advancing the phase of activation from that during steady-state flight may generate additional mechanical power output by enabling a larger percentage of the DLM_1 to function as a motor.

Given an inherent temperature gradient, the ability of the nervous system to control the phase of activation may in fact enhance the roles that the power muscles can play in neuromechanical control of locomotion. Surprisingly, operation at submaximal levels of power output may occur among flying, swimming, and terrestrial organisms (Josephson, 1997; Tu and Daniel, 2004b; S. Sponberg and T. L. Daniel, unpublished). Perhaps this energy conservation leaves reserves available to the organism for use in locomotor control or in extreme behaviors such as escape maneuvers. With a temperature gradient in place, an organism could simply shift the phase of activation to increase the proportion of muscle acting as a motor rather than an energy storage source or damper. Thus, given a fixed temperature gradient, an organism could modulate the phase of activation and thereby diversify the functional gradients accessible, effectively increasing the performance range.

3.5.5 Conclusions

A spatial gradient in the mechanical power output driven by a temperature gradient reveals a considerable spatial gradient in the functional consequences of simultaneous muscle activation in a single muscle. Our work-loop analyses show that the separate subunits of the DLM_1 concurrently operate as a power generator, an elastic energy storage source, or an energy absorber. Thus, the common assumption that the individual components of a muscle operate uniformly to command a single function should be re-evaluated in the context of measured spatial profiles of temperature. In addition to our current study, a growing body of evidence indicates that a single muscle can exhibit functional heterogeneity driven by morphological, neurological, and/or physiological differences (Mu and Sanders, 2001; Ahn and Full, 2002; Ahn et al., 2003; Higham et al., 2008; Wakeling, 2009). The subunits of the DLM_1 may function synergistically during flight, but this function may include elastic energy storage and damping in addition to the canonical view of power production. Although it has not been extensively studied in other organisms, significant temperature gradients in any locomotor muscle would necessarily imply a gradient in the functional roles played by regions within a single muscle.

3.6 List of abbreviations

DLM_1 dorsolongitudinal muscles
DLM_{1V} ventral subunits
DLM_{1D} dorsal subunits

3.7 Acknowledgements

We would like to thank Tom Irving, Emily Carrington, Ray Huey, Dave Williams, Armin Hinterwirth, Brad Dickerson, and Octavio Campos for their contributions. This material is based upon work supported by the National Science Foundation Graduate Research Fellowship [under grant no. DGE-0718124 to N.T.G.], an National Science Foundation Postdoctoral Fellowship in Biology [award no. 0905944 to S.S.], an National

Science Foundation Grant [IOS-1022471 to T.L.D.] and the University of Washington Komen Endowed Chair [T.L.D.]

Chapter 4

THE CROSS-BRIDGE SPRING: COOL MUSCLES STORE ELASTIC ENERGY

Nicole T. George, Charles D. Williams, Thomas C. Irving, and
Thomas L. Daniel

4.1 Abstract

Minimizing the energetic cost of muscle contraction is necessary to sustain locomotion. Significant energy savings have been associated with non-muscle structures such as tendon and cuticle, but recent studies document energy storage also occurs in extensible myofilaments. Here we examine whether intramuscular temperature gradients (which induce spatial gradients in force, energy, and molecular organization) additionally enables cross-bridges to store elastic energy. To monitor the movement of cross-bridges and force production in real time, we used time-resolved small-angle X-ray diffraction paired with mechanical work-loop tests, on an *in situ* preparation of *Manduca sexta*. This allowed us to couple whole-muscle mechanical behavior to molecular events. A 5-frame X-ray diffraction movie enabled us to visualize molecular and structural determinants of the temperature dependence of cross-bridge cycling and to evaluate the role of cross-bridges in elastic energy storage. Changes in the equatorial intensities, an indication of cross-bridge association with myofilaments, revealed that a temperature gradient likely creates a locked-spring lattice in

the cooler region of muscle. Cross-bridges in that region that remain bound and elastically deformed at the end of muscle shortening could release the stored strain energy during muscle lengthening. Our results have widespread implications for the complexity of muscle function and energy saving mechanisms.

4.2 Introduction

Elastic energy storage is widely recognized as a critical design characteristic of animal movement, as it promotes efficient and high-frequency locomotion. Canonical examples of elastic energy storage sites include the tendons of ankle extensor muscles in mammals and resilin, the rubber-like protein in insect cuticle (Jensen and Weis-Fogh, 1962; Alexander, 1984; Biewener et al., 1998; Patek et al., 2011). Elastic energy storage is believed to be particularly important to flying insects, significantly reducing the inertial power costs of accelerating the wings (Alexander and Bennet-Clark, 1977; Ellington, 1984; Dickinson and Lighton, 1995). Two main sites of elastic energy storage have been proposed for insect flight: in cuticular resilin (Jensen and Weis-Fogh, 1962; Burrows et al., 2008) and in extensible myofilaments [e.g. in the long axis of the thick and thin filaments (Huxley et al., 1994; Dickinson et al., 2005), cross-bridges, collagen fibrils (Tidball and Daniel, 1986; Dobbie et al., 1998), and in titin (Nishikawa et al., 2011)]. Here we propose that an intramuscular temperature gradient, by inducing a subsequent mechanical gradient, forms a regional locked-spring lattice capable of storing energy in the deformation of cross-bridges. A temperature gradient throughout an animal's musculature is an inevitable consequence of metabolic heat production combined with convective and radiative heat loss (George and Daniel, 2011). Cross-bridge cycling dynamics likely vary significantly along the muscles' temperature gradient, with high turnover rates in the warmer region of muscle but reduced cross-bridge cycling in the cooler region. Thus, cross-bridges in the cooler region of muscle will be less able to detach from their actin binding sites throughout the contraction cycle, potentially forming a locked-spring lattice. Elastic energy stored in cross-bridges that remain bound and elastically deformed at the end of the first half of the contraction cycle could be released during the second half, thus serving as an elastic restoring force on the cuticle and aiding in wing acceleration.

We use time-resolved small-angle X-ray fiber diffraction methods to monitor changes in mass distribution, which reflects the radial position of cross-bridges and, by implication, their association with the thin filaments. By pairing this visualization technique with simultaneous force and length measurements under controlled muscle activation, we were able to couple molecular observations with mechanical measures of whole muscle performance. We documented these events in *Manduca sexta*, a large moth known to have a significant dorso-ventral temperature gradient in its dominant flight muscle, the dorsolongitudinal muscle (DLM_1; George and Daniel, 2011). The DLM_1 was cyclically oscillated and periodically stimulated at 25 Hz (normal wingbeat frequency) while recording force and length, establishing a "work-loop" that measures the cyclic mechanical energy input or output of activated muscles (*sensu* Josephson, 1985; Fig. 4.1). Here we show how a spatial gradient in muscle temperature affects the regional cycling dynamics of cross-bridges. We conducted work-loop experiments at two muscle temperatures, 25ºC and 35ºC, to encompass the hot and cold range of *M. sexta's* temperature gradient (Fig. 4.2; George and Daniel, 2011). Additionally, to test for the regional specialization of contractile dynamics, we focused the X-ray beam on either a ventral or a dorsal location of the DLM_1. X-ray diffraction patterns were collected with a time resolving (250 Hz frame rate), photon-counting detector (PILATUS 100K, Dectris, Ltd.) at five specific time points (every 8 ms with 4 ms exposures) during each of the 40 ms cyclic contractions. Diffraction patterns were cycle averaged across 80 cycles to create a final movie of 5 averaged frames. From this diffraction movie, we measured the cyclical changes in lattice spacing and intensities of the 2,0, 1,1, and 1,0 equatorial reflections, ($I_{2,0}$, $I_{I,1}$ and $I_{1,0}$; Fig. 4.2). We tracked lattice spacing by measuring the distance from the center of the diffraction pattern to the 1,0 reflection. This was then converted to the d_{10} lattice spacing, the distance between myofilaments, as in Irving, 2006 (Irving, 2006). The ratio of $I_{1,1}+I_{2,0}$ to $I_{1,0}$, "the equatorial intensity ratio", estimates the association of cross-bridges with the thin filament; a higher ratio indicates a shift in cross-bridge mass towards the thin filament. We expected the warmer ventral region of the DLM_1 to behave as the main power generator and therefore to high cross-bridge turnover. But if the cool dorsal region of muscle behaves as a locked-spring lattice, then a portion of cross-bridges would remain stably bound to the thin filaments, thereby restraining radial expansion and enabling elastic energy storage.

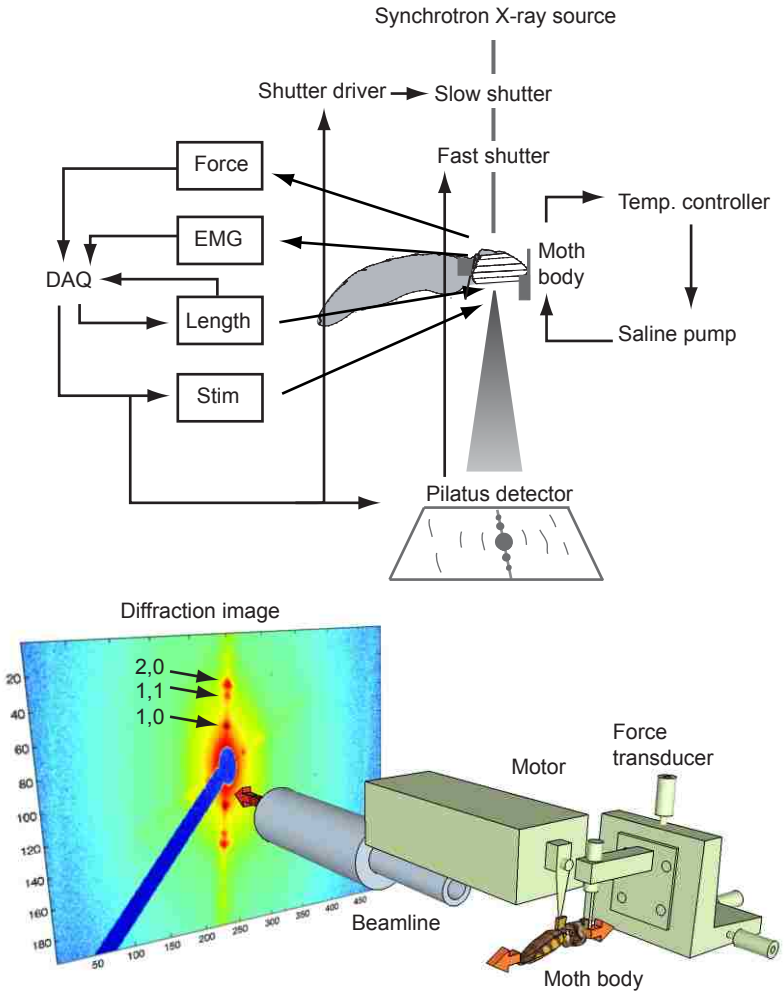

Figure 4.1: X-ray diffraction and work-loop preparation. *Manduca sexta* (head, legs, and wings removed) was fixed in a work-loop apparatus such that the DLM_1 was isolated between a motor and a rigid force transducer. The muscle was cyclically oscillated at 25 Hz while being electrically stimulated at the *in vivo* phase of activation. Concurrently, we monitored the movement of cross-bridges in real time with synchrotron small-angle X-ray diffraction. X-rays passed through the oscillating DLM_1 at 5 specific equally spaced time points throughout the contraction cycle. The corresponding diffraction pattern is characteristic of the periodic array of the thick and thin filaments. The 2,0, 1,1, and 1,0 equatorial reflections arise from the spacing between myofilaments, and are therefore related to the mass distribution of the cross-bridges.

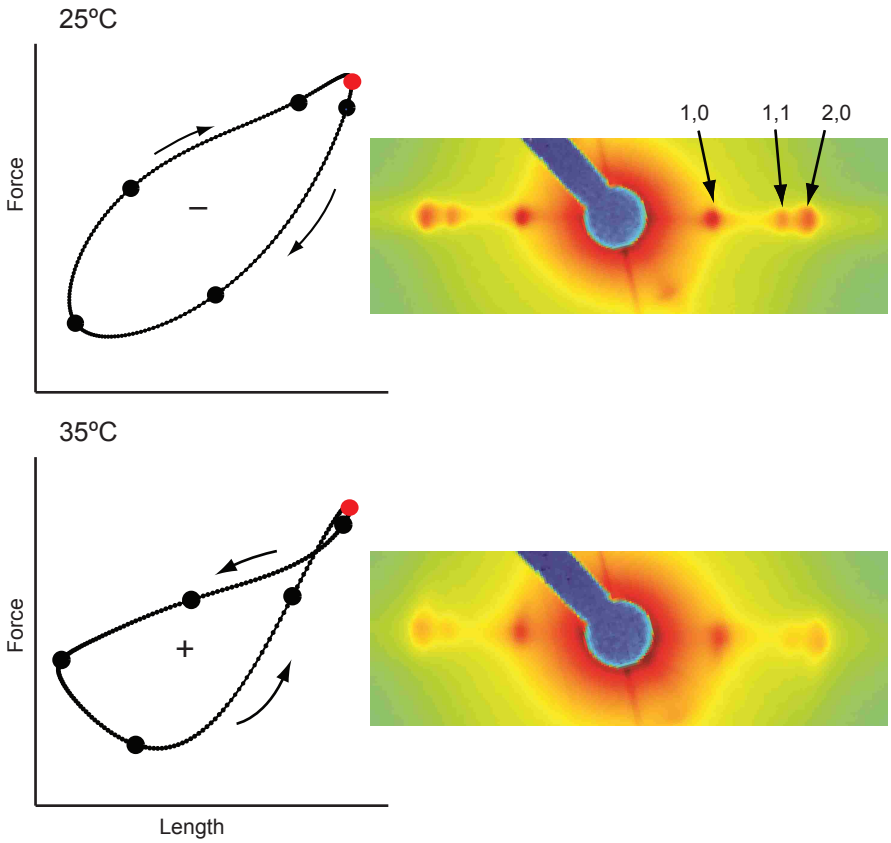

Figure 4.2: An example negative work-loop at 25ºC and positive work-loop at 35ºC. The red dot indicates the point of muscle activation and the black dots represent when diffraction images were collected throughout the contraction cycle. Net work is calculated by integrating force output with respect to muscle length. Mass specific power output is then calculated as the sum of cycle frequency (25 Hz) and net work divided by muscle mass. On the right, concurrent diffraction images from the time point directly following muscle stimulation (represented by the red dot) highlight the temperature dependent variation in the lattice structure. The temperature dependent change in lattice spacing is present as a difference in the distance between opposing 1,0 equatorial reflections and the variation in cross-bridge mass shift is present in the change in relative intensities of the 1,0, 1,1, and 2,0 equatorial reflections.

4.3 Results

4.3.1 Operating conditions

The 5 moths (2 males and 3 females) used in these trials had a mean body mass of 2.50±0.17 g and a mean extracted DLM_1 mass of 0.206±0.009 g (s.d). The mean rest length of the mesothorax was 10.07±0.14 mm (s.d.), which set the mean operating mesothorax length at 9.86±0.14 mm (s.d.). The mean peak-to-peak strain amplitude imposed by the motor on the DLM_1 was 0.63±0.02 mm (s.d.), with only 1.1% strain amplitude variation across individuals. The DLM_1 were electrically stimulated at the *~in vivo* phase of activation, 0.51±0.01 (0.49±0.04; Tu and Daniel, 2004a).

4.3.2 Effect of temperature on cross-bridge cycling dynamics

Mean power output of the DLM_1 depends strongly on temperature. At 35ºC, mean mechanical power output was 42.98±1.62 W kg^{-1}. In contrast, power output at 25ºC was significantly negative, with a mean of –161.20±3.20 W kg^{-1} (n=5 moths, mean ± SEM; t-test, P<0.0001; Fig. 4.2). These values are consistent with mechanical power output measured at the *in vivo* phase of activation in prior work-loop studies with *M. sexta* (Tu and Daniel, 2004b; George et al., 2012).

Consistent with observed variation in power output at 25ºC and 35ºC, lattice spacing and cross-bridge cycling dynamics were also significantly temperature dependent. For a comparison of the effect of temperature on these two factors, we highlight results from the biologically relevant condition, the ventral region of the DLM_1 at 35ºC versus the dorsal region of the DLM_1 at 25ºC (George and Daniel, 2011). The relationship between temperature and myofilament lattice spacing, as indicated by the d_{10}, is shown throughout the contraction cycle in Fig. 4.3A. Although there was no significant difference in lattice spacing throughout the contraction cycle for muscle at 25ºC and 35ºC, there was a significant difference due to muscle temperature [repeated-measures analysis of variance (ANOVA): effect of time $F(4.36)=1.3$, $P=0.29$; effect of temperature $F(1,36)=13.1$, $P<0.001$]. Because there was no effect of time, we combined the results for each temperature and found that

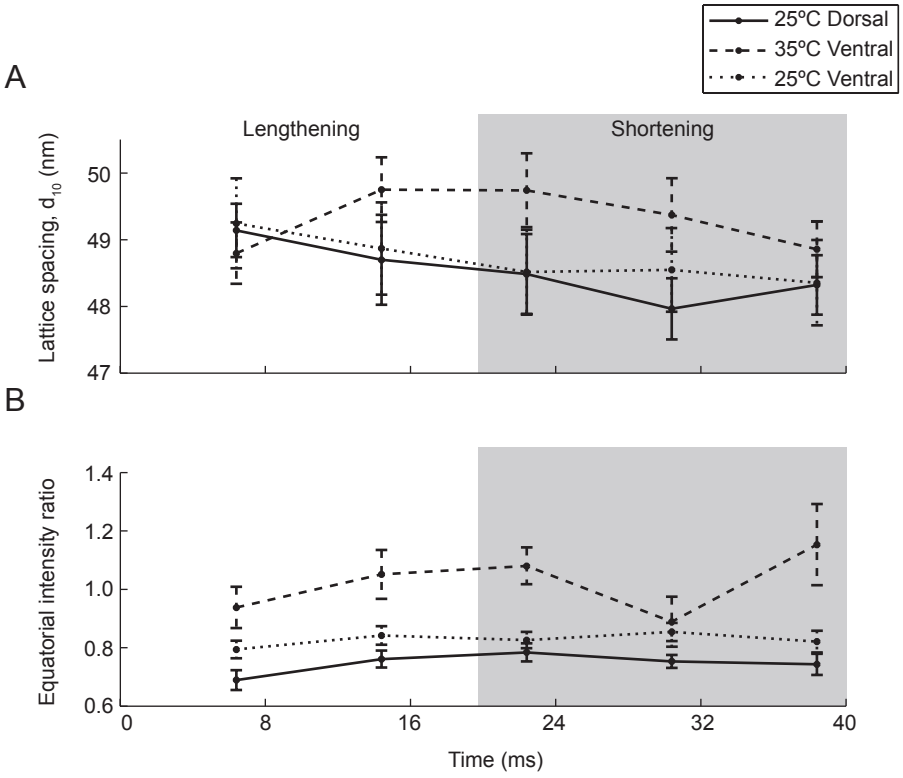

Figure 4.3. Variation in lattice structure throughout the contraction cycle (40 ms in duration; *n*=5 moths). The non-shaded and shaded areas indicate the lengthening and shortening phase of the cycle, respectively. (A) Lattice spacing, as determined by the d_{10}, is plotted as a function of the contraction cycle for dorsal muscle at 25ºC, ventral muscle at 35ºC, and ventral muscle at 25ºC. Across the 5 time points, mean lattice spacing was significantly lower in 25ºC muscle than in 35ºC muscle, regardless of muscle location. (B) Equatorial intensity ratio, calculated by $(I_{1,1}+I_{2,0})/I_{1,0}$, as a function of the contraction cycle. Although muscle at 35ºC showed the expected cyclic response in the intensity ratio, muscle at 25ºC had an uncharacteristically stable and uniform response. Once again, the similar response of both locations at 25ºC indicates that dorsal muscle is not specialized to operate at the lower temperature in terms of its contractile dynamics. Error bars show standard errors of the mean.

lattice spacing was lower on average in cold dorsal muscle, such that myofilaments were ~0.8 nm closer together than in warm ventral muscle (t-test, $P<0.01$). It is possible that cross-bridges in cooler muscle have a reduced ability to detach from the thin filaments throughout the cycle, thus limiting the mobility of the lattice and preventing regular changes in radial spacing.

As in cardiac muscle, the restrained filament lattice in cold muscle also appears to correspond with a comparatively low equatorial intensity ratio throughout the cycle (Fig. 4.3B) (Farman et al., 2011; Perz-Edwards et al., 2011). The intensity ratio was significantly affected by both temperature and time point in the contraction cycle [repeated-measures ANOVA: effect of time $F(4,32)=3.1$, $P<0.05$; effect of temperature $F(1,8)=14.1$, $P<0.01$]. The intensity ratio across the whole contraction cycle averaged 37% higher in 35ºC ventral muscle than in 25ºC dorsal muscle (*t*-test, $P<0.0001$). The equatorial intensity ratio reflects the mass shift of cross-bridges as they move away from the thick filament towards the thin filament; higher ratios reflect increased radial extension, presumably associated with acto-myosin interaction. Therefore, the higher overall intensity ratio in warm muscle may also be ascribed to the elevated cross-bridge activity expected of a power producing muscle. Figure 3B also beautifully demonstrates the cyclical change in cross-bridge mass distribution expected of warm muscle (note the large fluctuation in the intensity ratio during the second half of the cycle), versus the stable, uniform binding expected of a locked-spring lattice in cooler muscle. This is indicated by the larger absolute percent change in the intensity ratio between progressive points in the cycle in warm muscle (mean = 17%, maximum = 29%), than in cool muscle (mean = 7%, maximum = 11%). Taken together, these data indicate that some cross-bridges in the cooler region of muscle remain bound to the thin filaments throughout the contraction cycle, thus maintaining a locked-spring lattice.

4.3.3 Effect of muscle location

In addition, we controlled for the effect of location and determined that the subregions of the DLM_1 are not regionally specialized for local temperature in terms of their contractile dynamics. Diffraction patterns from the ventral and dorsal locations at the same respective temperature, 25ºC or 35ºC, did not show sufficient variation to indicate that the DLM_1

employs physiological compensatory mechanisms to account for the effect of a temperature gradient on regional contractile rates. Lattice spacing was not significantly different between dorsal and ventral muscle at 25ºC or at 35ºC (two-way ANOVA, P=0.63 at 25ºC and P=0.45 at 35ºC; Fig. 4.3A). Myofilament spacing was likewise more restrained in ventral muscle at cold temperatures than at warm temperatures (~0.6 nm less; paired t-test, P<0.01). Although there was an effect of location on the intensity ratio at 25ºC and 35ºC (two-way ANOVA, P<0.001 at 25ºC and P<0.01 at 35ºC), the overall response, cyclic cross-bridge binding at 35ºC versus uniform cross-bridge activity at 25ºC, was comparable between locations, indicating no effective regional specialization in molecular cycling dynamics (Fig. 4.3B).

4.4 Discussion

The cyclical changes in the intensities and positions of major reflections in the well-ordered filament lattice of *M. sexta* indicate that a temperature gradient likely induces spatially specific and functionally distinct cross-bridge cycling dynamics within a single muscle. Furthermore, the spatial variation in cross-bridge turnover rates appears to form a locked-spring lattice within the cooler region of muscle that is capable of storing and releasing energy.

Temperature gradients within a single muscle inevitably result from the balance between metabolic heat production and surface heat loss from convective and radiative cooling. Because muscle physiological properties are temperature dependent, this gradient has significant implications for muscle power production and functional output (Josephson, 1984; Bennett, 1985; George and Daniel, 2011; George et al., 2012). The DLM_1 of *M. sexta* has been generally presumed to operate solely as an actuator, producing positive power to indirectly accelerate the wings downwards. However, our mechanical tests clearly demonstrate that because of a significant temperature gradient, power output varies regionally from positive values (warm sectors) to negative values (cool sectors) within this single muscle. We found that the observed variation in contractile dynamics are responsible for this decrease in power production and may provide a mechanism by which cross-bridges could contribute stored elastic energy to the overall energy needed for flight.

Concurrently while the warm ventral region of muscle dictates the high-frequency

motion of flight, reduced contractile rates in the cooler dorsal region would create a lattice that is restrained by cross-bridges, which are less able to detach from their actin binding sites. Thus, the cool dorsal region could form a locked-spring lattice that may store elastic energy in axial extensions of the filaments as well as in axial and radial extensions of cross-bridges. Our data support this hypothesis by the overall reduced lattice spacing and uncharacteristic, temporally uniform, intensity ratio observed in cold muscle. Elastic energy stored in cross-bridges that remain bound and deformed at the end of the shortening phase of the contraction cycle could then be released during the lengthening phase of the cycle. In doing so, the deformed cross-bridges could aid the antagonistic muscle by acting as a restoring force. Prior studies have determined that elastic energy storage is crucial towards meeting the high inertial power costs of flight (Alexander and Bennet-Clark, 1977; Ellington, 1984; Dickinson and Lighton, 1995). If even a portion of these cross-bridges could facilitate elastic energy savings via a temperature gradient, they would contribute to the overall energetic requirements and improve locomotor efficiency. Because temperature gradients may be an inevitable consequence of internal energy generation and heat dissipation, this mechanism of energy storage may a general phenomenon in locomotor systems.

4.5 Materials and methods

4.5.1 Moths

Manduca sexta (L.) were raised in a colony maintained by the Department of Biology at the University of Washington, Seattle, WA, USA. After eclosion, moths were kept in light for 24 h. Moths were used within 5 days of eclosion. Prior to experimental preparation moths were immobilized by cold (~4ºC).

4.5.2 Work-loop preparation

Work-loop methods are as previously described in George et al., 2012. In brief, the DLM_1 of *M. sexta* was subjected to sinusoidal length changes and phase-specific stimulation, while force output and length were recorded to calculate net work. *M. sexta* were mounted in the

work-loop apparatus, such that just the DLM_1 was isolated between a rigid force transducer (Fort100, WPI, Sarasota, FL, USA) and a motor lever arm (Model 305B Dual-Mode Lever Arm System, Aurora Scientific Inc., Aurora, ON, Canada). The muscle was electrically stimulated and sinusoidally oscillated at 25 Hz for 2 s. Two tungsten electrodes (~10 mm long) connected to a stimulator and driven through the DLM_1 (Isolator Pulse Stimulator Model 2100, A-M Systems, Sequim, WA, USA) delivered 0.4 ms supramaximal stimuli at the *in vivo* phase of activation, ~0.51 of the length cycle (Tu and Daniel, 2004a). The phase of activation was calculated as the duration of time from the start of muscle lengthening to the subsequent evoked potential as a fraction of the complete cycle duration (40 ms). The evoked potentials were recorded with a bipolar differential tungsten electrode inserted in the DLM_1 and a common reference wire placed in the abdomen. The signal was amplified (x1000) with a differential AC amplifier (Model 1800, A-M Systems, Sequim, WA, USA) and band pass filtered (300-20KHz). The induced peak-to-peak strain amplitude was ~0.6 mm (~±3% of the initial muscle length), with a duty factor of ~0.5 (the fraction of time spend shortening during the length cycle). The large inertial mass of *M. sexta's* body oscillating on the motor limited us to impose a strain only a fraction, ~60%, of the *in vivo* strain (Tu and Daniel, 2004a). To test for the effect of temperature, a heated *M. sexta* saline (Lei et al., 2004) drip system maintained the muscle temperature at either 25 or 35ºC. The drip system included a temperature regulator (Bipolar Temperature Controller Model CL-100, Warner Instruments, Hamden, ST, USA), a cooling unit (Thermal Cooling Module Model TCM-1, Warner Instruments, Hamden, CT, USA), a pump (Masterflex C/L Model 77120-62, Cole-Palmer, Vernon Hills, IL, USA) and a drip emitter (In-line Heater/Cooler Model SC-20, Warner Instruments, Hamden, CT, USA).

Net work per cycle was calculated by integrating force output with respect to muscle length. For each experimental condition, we calculated the net work for 20 cycles, starting with the 10^{th} cycle. Mass specific power output is the product of mean net work and cycle frequency (25 Hz, normal wingbeat frequency) divided by the mass of the DLM_1. We determined the mass of the DLM_1 by extracting the muscle from the thorax while immersed in *M. sexta* saline directly after experimentation. The DLM_1 was then blotted and weighed to the nearest 0.1 mg. Power output by the DLM_1 was not confounded by a decrease in performance over the ~10 min experiment period due to fatigue. A prior work-loop study on

M. sexta found no significant difference in power output after 20 min of work-loop testing under similar conditions (George et al., 2012).

4.5.3 X-ray diffraction

Time-resolved X-ray diffraction patterns were collected using the small-angle diffraction instrument on the Biophysics Collaborative Access Team beamline 18 ID at the Advanced Photon Source, Argonne National Laboratory. The work-loop apparatus (previously described in George et al., 2012) was positioned to hold the preparation in the direct line of the X-ray beam, 2.945 m from the PILATUS 100K detector (Dectris, Ltd.). The X-ray beam contained ~1 x 10^{13} photons per second at 12 keV beam energy and was collimated to about 250 x 250 μm at the sample position and focused to ~50x150 μm at the detector. The stimulus signal sent to the DLM_1 also triggered the shutter driver acting as a gate and delay generator (Model VMM-T1, Uniblitz, Rochester, NY, USA) to open the slow x-ray shutter (model PFCU/PF4/PFS2 XIA LLC Hayward CA). A custom made fast shutter (~1 ms latency, < 1ms minimum opening time), gated by the PILATUS integration signal was triggered to open every 8 ms (with 4 ms exposures) of the 40 ms wingbeat cycle, yielding a total of 5 diffraction images per cycle for 100 cycles. This essentially produced a diffraction movie of a 125 frames/s with each frame representing the phase-sensitive structure of the contractile unit. The stage holding the work-loop apparatus was attached to a motor driven unit that rastered the sample horizontally (± 2 mm) at ~0.5 m/s during the X-ray exposure to limit the amount of radiation a single point in the muscle fiber received. In addition to testing for the effect of temperature, we also compared the effect of DLM_1 subunit location. The sample was positioned such that the X-rays were incident on one of two locations, a dorsal and a ventral region of the DLM_1.

4.5.4 Diffraction pattern analysis

For each condition, 400 images were averaged across the corresponding phases of the length cycle to yield one cycle of 5 diffraction images, significantly improving the signal-to-noise ratio of the image. When cross-bridges move from the region of the thick filament backbone

to that of the thin filament, there is an increase in the mass along the 2,0 and 1,1 crystallographic plane (primarily thin filaments) and a reduction in mass along the 1,0 plane (primarily thick filaments). As such, the ratio of the intensities of the 2,0 + 1,1, and 1,0 equatorial reflections ($I_{1,1}+I_{20}/I_{10}$) can be used as a measure of the radial position of cross-bridges relative to the thick and thin filament (Fig. 4.1). A higher intensity ratio is reflective of cross-bridges being more associated with, and presumably bound to, the thin filaments (Miller and Tregear, 1970; Irving, 2006)

Using custom written software in Python, we determined the intensities of the 2,0, 1,1 and 1,0 reflections ($I_{2,0}$, $I_{1,1}$, and $I_{1,0}$), by first integrating the intensities orthogonal to the equatorial line. An exponential fit based on manually selected points along the baseline removed the diffuse background. The area under the one dimensional projection of the $I_{2,0}$, $I_{1,1}$, and $I_{1,0}$ was then calculated by peak fitting (Fityk; Wojdyr, 2010) assuming a Gaussian shape and the peak positions constrained to be at the expected reciprocal lattice positions and peak widths constrained as described by Yu et al. (Yu et al., 1985). Briefly, the width of the Gaussian representing a given diffraction peak σ_{hk} can be expressed as:

$$\sqrt{\sigma_c^{\,2} + \sigma_d^{\,2} S_{hk} + \sigma_s^{\,2} S_{hk}^{\,2}},$$

where $S_{hk} = \sqrt{h^2 + k^2 + hk}$ and h and k are the Miller indices of the diffraction peak. σ_c is the known width of the X-ray beam (~ 1 pixel), σ_d is related to the amount of heterogeneity in inter-filament spacing among the myofibrils, and σ_s is related to the amount of paracrystalline (liquid-like) disorder of the myofilaments in the hexagonal lattice. Both σ_d and σ_s are used as free parameters of the fits. If the cool dorsal region of the muscle behaves as a locked-spring lattice we would expect that the cross-bridges are on average more associated with the thin filament throughout the contraction cycle. In contrast, we expect warmer ventral muscles to behave as the main power generators and therefore have greater cross-bridge turnover. This would correspond with a comparatively stable intensity ratio in cool muscle versus the expected periodic fluctuation in warm muscle. Additionally, we were able to track lattice spacing by measuring the distance between the 1,0 reflection and the center of the pattern. This was converted to the d_{10} lattice spacing, the distance between myofilaments, as in Irving, 2006.

4.5.5 Data acquisition

Force, muscle length, evoked potentials, and shutter exposures were recorded at 5000 Hz by a data acquisition system (NI USB-6229, National Instruments, Austin, TX, USA) and relayed to a central processing unit. Evoked potentials were analyzed using custom peak detection software in MATLAB developed by M. S. Tu (University of Washington, Seattle, WA, USA).

4.7 Acknowledgements

We would like to thank Emily Carrington, Ray Huey, Armin Hinterwirth, Simon Sponberg, and Mary Salcedo for their contributions. This material is based upon work supported by the National Science Foundation Graduate Research Fellowship under Grant No. DGE-0718124 to N.T.G., an NSF Grant (IOS-1022471) to T.L.D and T.C.I. and the University of Washington Komen Endowed Chair to T.L.D.

BIBLIOGRAPHY

Ahn, A. N. and Full, R. J. (2002). A motor and a brake: two leg extensor muscles acting at the same joint manage energy differently in a running insect. *J. Exp. Biol.* **205**, 379-89.

Ahn, A. N., Monti, R. J. and Biewener, A. A. (2003). *In vivo* and *in vitro* heterogeneity of segment length changes in the semimembranosus muscle of the toad. *J. Physiol*. **549.3**, 877-888.

Alexander, R. M. and Bennet-Clark, H. C. (1977). Storage of elastic strain energy in muscle and other tissues. *Nature* **265**, 114-117.

Alexander, R. M. (2003). Principles of Animal Locomotion. Princeton University Press: Princeton.

Alexander, R. M. (1984). Elastic Energy Stores in Running Vertebrates. *Integ. Comp. Biol*. **24**, 85-94.

Altringham, J. D., Wardle, C. S., and Smith, C. I. (1993). Myotomal muscle function at different locations in the body of a swimming fish. *Stimulus*. **206**, 191-206.

Altringham, J. D. and Ellerby, D. J. (1999). Fish swimming: patterns in muscle function. *J. Exp. Biol.* **202**, 3397-3403.

Altringham, J. D. and Johnston, I. A. (1990). Scaling effects on muscle function: power output of isolated fish muscle fibers performing oscillatory work. *J. Exp. Biol.* **151**, 453-467.

Azizi, E. and Roberts, T. J. (2009). Biaxial strain and variable stiffness in aponeuroses. *J. Physiol.* **587**, 4309-18.

Bennett, A. F. (1985). Temperature and muscle. *J. Exp. Biol.* **115**, 333-344.

Bennett, A. F. (1984). Thermal dependence of muscle function. *Am. J. Physiol.* **247**, R217-29.

Biewener, A. A. (1998). Muscle-tendon stresses and elastic energy storage during locomotion in the horse. *Comp. Biochem. and Physiol. Part B* **120**, 73-87.

Biewener, A. A., Konieczynski, D. D., and Baudinette, R. V. (1998). In vivo muscle force-length behavior during steady-speed hopping in tammar wallabies. *J. Exp. Biol.* **201**, 1681-94.

Burrows, M., Shaw, S. R., and Sutton, G. P. (2008). Resilin and chitinous cuticle form a composite structure for energy storage in jumping by froghopper insects. *BMC Biol.* **6**, 41.

Carey, F. G. and Teal, J. M. (1966). Heat conservation in tuna fish muscle. *Proc. Natl. Acad. Sci. USA* **56**, 1464-1469.

Coelho, J. R. (1991). The effect of thorax temperature on force production during tethered flight in honeybee (*Apis mellifera*) drones, workers, and queens. *Physiol. Zool.* **64**, 823-835.

Dickinson, M. H. and Lighton, J. R. B. (1995). Muscle efficiency and elastic storage in the flight motor of *Drosophila*. *Science* **268**, 87-90.

Dickinson, M. H., Farley, C. T., Full, R. J., Koehl, M. A., Kram, R., and Lehman, S. (2000). How animals move: an integrative view. *Science* **288**, 100-106.

Dickinson, M., Farman, G., Frye, M., Bekyarova, T., Gore, D., Maughan, D., and Irving, T. (2005). Molecular dynamics of cyclically contracting insect flight muscle in vivo. *Nature* **433**, 330-4.

Dobbie, I., Linari, M., Piazzesi, G., Reconditi, M., Koubassova, N., Ferenczi, M. A., Lombardi, V., and Irving, M. (1998). Elastic bending and active tilting of myosin heads during muscle contraction. *Nature* **396**, 383-387.

Eaton, J. L. (1988). Lepidopteran Anatomy. John Wiley & Sons: New York.

Ellington, C. P. (1985). Power and efficiency of insect flight muscle. *J. Exp. Biol.* **115**, 293-304.

English, A. W., Wolf, S. L., and Segal, R. L. (1993). Compartmentalization of muscles and their motor nuclei: the partitioning hypothesis. *Phys. Ther*. **73**, 857-67.

Farman, G. P., Gore, D., Allen, E., Schoenfelt, K., Irving, T. C., and de Tombe, P. P. (2011). Myosin head orientation: a structural determinant for the Frank-Starling relationship. *Am. J. Physiol.* **300**, H2155-60.

Full, R. J., Stokes, D. R., Ahn, A. N., and Josephson, R. K. (1998). Energy absorption during running by leg muscles in a cockroach. *J. Exp. Biol.* **201** (Pt 7), 997-1012.

George, N. T., Sponberg, S., and Daniel, T. L. (2012). Temperature gradients drive mechanical energy gradients in the flight muscle of Manduca sexta. *J. Exp. Biol.* **215**, 471-9.

George, N. T. and Daniel, T. L. (2011). Temperature gradients in the flight muscles of Manduca sexta imply a spatial gradient in muscle force and energy output. *J. Exp. Biol.* **214**, 894-900.

Gordon, A. M., Huxley, A. F., and Julian, F. J. (1966). The variation in isometric tension with sarcomere length in vertebrate muscle fibres. *J. Physiol.* **184**, 170-92.

Gosline, J., Lillie, M., Carrington, E., Guerette, P., Ortlepp, C., and Savage, K. (2002). Elastic proteins: biological roles and mechanical properties. *Phil. Trans. R. Soc. Lond. B* **357**, 121-32.

Haas, F., Gorb, S., and Blickhan, R. (2000). The function of resilin in beetle wings. *Proc. R. Soc. Lond. B* **267**, 1375-81.

Heinrich, B. (1995). Insect thermoregulation. *Endeavour*, **19,** 28-33.

Heinrich, B. (1971). Temperature regulation in the sphinx moth, Manduca sexta: I. Flight energetics and body temperature during free and tethered flight. *J. Exp. Biol.* **54**, 141-152.

Heinrich, B. (1974). Thermoregulation in endothermic insects. *Science* **185**, 747-56.

Heinrich, B. and Casey, T. M. (1972). Metabolic rate and endothermy in sphinx moths. *J. Comp. Physiol.* **82**, 195-206.

Higham, T. E. and Biewener, A. A (2008). Integration within and between muscles during terrestrial locomotion: effects of incline and speed. *J. Exp. Biol.* **211**, 2303-16.

Higham, T. E., Biewener, A. A, and Wakeling, J. M. (2008). Functional diversification within and between muscle synergists during locomotion. *Biol. Lett.* **4**, 41-4.

Hill, A. (1938). The heat of shortening and the dynamic constants of muscle. *Proc. R. Soc. Lond. B* **126**, 136–195.

Hoffer, J. A., Loeb, G. E., Sugano, N., Marks, W. B., O'Donovan, M. J., and Pratt, C. A. (1987). Cat hindlimb motorneurons during locomotion. III. Functional segregation in sartorius. *J. Neurophysiol.* **57**, 554-562.

Holtermann, A., Roeleveld, K., and Karlsson, J. S. (2005). Inhomogeneities in muscle activation reveal motor unit recruitment. *J. Electromyogr. Kinesiol.* **15**, 131-7.

Huxley, H. E., Stewart, A., Sosa, H., and Irving, T. (1994). X-ray diffraction measurements of the extensibility of actin and myosin filaments in contracting muscle. *Biophys. J.* **67**, 2411-21.

Irving, T. C. (2006). X-ray Diffraction of Indirect Flight Muscle from *Drosophila in vivo (*in *Nature's Versatile Engine: Insect Flight Muscle Inside and Out,* J Vigoreaux) editor Landes Biosciences, Georgetown, TX.

Janiszewski, J. (1984). The temperature of the head, thorax and abdomen of Periplaneta americana during rest and flight at high ambient temperatures. *J. Therm. Biol.* **9**, 177-181.

Jensen, M. and Weis-Fogh, T. (1962). Biology and Physics of Locust Flight . V . Strength and Elasticity of Locust Cuticle Source. *Phil. Trans. R. Soc. Lond. B.* **245**, 137-169.

Johnson, T. P. and Johnston, I. A. (1990). Temperature adaptation and the contractile properties of live muscle fibers from teleost fish. *J. Comp. Physiol. [B]* **161**, 27-36.

Johnson, T. P. and Johnston, I. A. (1991). Power output of fish muscle fibers performing oscillatory work: effects of acute and seasonal temperature change. *J. Exp. Biol.* **157**, 409-423.

Jones, D. A., Round, J. M., and Haan, A. D. (2004). Skeletal muscle from molecules to movement: A textbook of muscle physiology for sport, exercise, physiotherapy, and medicine. Churchill Livingstone: Edinburgh.

Josephson, R. K. (1993). Contraction dynamics and power output of skeletal muscle. *Ann. Rev. Physiol.* **55**, 527-46.

Josephson, R. K. (1999). Dissecting muscle power output. *J. Exp. Biol.* **202**, 3369-75.

Josephson, R. K. (1985). Mechanical power output from striated muscle during cyclic contraction. *J. Exp. Biol.* **114**, 493-512.

Josephson, R. K. and Stevenson, R. D. (1991). The efficiency of a flight muscle from the locust Schistocerca americana. *J. Physiol. Lond.* **442**, 413-29.

Josephson, R. K. (1984). Contraction dynamics of flight and stridulatory muscles of tettigoniid insects. *J. Exp. Biol.* **108**, 77-96.

Kammer, A. E. (1968). Motor patterns during flight and warm-up in Lepidoptera. *J. Exp. Biol.* **48**, 89-109.

Kier, W. M. and Curtin, N. A. (2002). Fast muscle in squid (Loligo pealei): contractile properties of a specialized muscle fibre type. *J. Exp. Biol.* **205**, 1907-16.

Kondoh, Y. and Obara, Y. (1982). Anatomy of motorneurons innervating mesothoracic indirect flight muscles in the silkmoth, *Bombyx mori*. *J. Exp. Biol.* **98,** 23-37.

Langfeld, K. S., Altringham, J. D., and Johnston, I. A. (1989). Temperature and the force-velocity relationship of live muscle fibers from teleost Myoxocephalus scorpius. *J. Exp. Biol.* **144**, 437-448.

Lei, H., Christensen, T. A., and Hildebrand, J. G. (2004). Spatial and temporal organization of ensemble representations for different odor classes in the moth antennal lobe. *J. Neurosci.* **24**, 11108-11119.

Marden, J. H. (1995). Evolutionary adaptation of contractile performance in muscle of ectothermic winter-flying moths. *J. Exp. Biol.* **198**, 2087-2094.

Marsh, R. L. and Olson, J. M. (1994). Power output of scallop adductor muscle during contractions replicating the in vivo mechanical cycle. *J. Exp. Biol.* **193**, 139-56.

Marsh, R. L., Olson, J. M., and Guzik, S. K. (1992). Mechanical performance of scallop adductor muscle during swimming. *Nature*. **357**, 411-413.

McCrea, M. J. and Heath, J. E. (1971). Dependence of flight on temperature regulation in the moth, Manduca sexta. *J. Exp. Biol.* **54**, 415-35.

McMahon, T. A. (1984). Muscles, reflexes and locomotion Princeton University Press: Princeton.

Miller, A. and Tregear, R. (1970). Evidence concerning crossbridge attachment during muscle contraction. *Nature* **226**, 1060-1061.

Monti, R. J., Roy, R. R., and Edgerton, V. R. (2001). Role of motor unit structure in defining function. *Muscle & Nerve*, **24**, 848-66.

Mu, L. and Sanders, I. R. A. (2001). Neuromuscular Compartments and Fiber-Type Regionalization in the Human Inferior Pharyngeal. *Anat. Rec.* **264**, 367-377.

Nishikawa, K. C., Monroy, J. A., Uyeno, T. E., Yeo, S. H., Pai, D. K., and Lindstedt, S. L. (2011). Is titin a " winding filament "? A new twist on muscle contraction. *Proc. R. Soc. B.*

Pappas, G. P., Asakawa, D. S., Delp, S. L., Zajac, F. E., and Drace, J. E. (2002). Nonuniform shortening in the biceps brachii during elbow flexion. *J. App. Physiol.* **92**, 2381-9.

Patek, S. N., Dudek, D. M., and Rosario, M. V. (2011). From bouncy legs to poisoned arrows: elastic movements in invertebrates. *J. Exp. Biol.* **214**, 1973-80.

Perz-Edwards, R. J., Irving, T. C., Baumann, B. A. J., Gore, D., Hutchinson, D. C., Kržič, U., Porter, R. L., Ward, A. B., and Reedy, M. K. (2011). X-ray diffraction evidence for myosin-troponin connections and tropomyosin movement during stretch activation of insect flight muscle. *Proc. Nat. Acad. Sci. USA* **108**, 120-5.

Rall, J. A and Woledge, R. C. (1990). Influence of temperature on mechanics and energetics of muscle contraction. *Am. J. Physiol.* **259**, R197-203.

Rassier, D. E., MacIntosh, B. R., and Herzog, W. (1999). Length dependence of active force production in skeletal muscle. *J. App. Physiol.*, **86**, 1445-57.

Roberts, T. J. (1997). Muscular Force in Running Turkeys: The Economy of Minimizing Work. *Science* **275**, 1113-1115.

Rome, L. C. and Swank, D. (1992). The influence of temperature on power output of scup red muscle during cyclical length changes. *J. Exp. Biol.* 171, 261-281.

Rome, L. C., Swank, D. M., and Coughlin, D. J. (1999). The influence of temperature on power production during swimming. II. Mechanics of red muscle fibres in vivo. *J. Exp. Biol.* **202**, 333-45.

Rome, L. C., Swank, D., and Corda, D. (1993). How fish power swimming. *Science* **261**, 340-343.

Sane, S. P. and Jacobson, N. P. (2006). Induced airflow in flying insects II. Measurement of induced flow. *J. Exp. Biol.* **209**, 43-56.

Scholle, H. C., Schumann, N. P., Biedermann, F., Stegeman, D. F., Graßme, R., Roeleveld, K., Schilling, N., and Fischer, M. S. (2001). Spatiotemporal surface EMG characteristics from rat triceps brachii muscle during treadmill locomotion indicate selective recruitment of functionally distinct muscle regions. *Exp. Brain Res.*, **138**, 26-36.

Sponberg, S., Libby, T., Mullens, C. H., and Full, R. J. (2011). Shifts in a single muscle's control potential of body dynamics are determined by mechanical feedback. *Phil. Trans. R. Soc. Lond. B* **366**, 1606-20.

Stevenson, R. D. and Josephson, R. K. (1990). Effects of operating frequency and temperature on mechanical power output from moth flight muscle. *J. Exp. Bio.l* **149**, 61-78.

Swank, D. M. and Rome, L. C. (2001). The influence of thermal acclimation on power production during swimming. II. Mechanics of scup red muscle under in vivo conditions. *J. Exp. Biol.* **204**, 419-30.

Swank, D. M., Zhang, G., and Rome, L. C. (1997). Contraction kinetics of red muscle in scup: mechanism for variation in relaxation rate along the length of the fish. *J. Exp. Biol.* **200**, 1297-307.

Swoap, S. J., Johnson, T. P., Josephson, R. K., and Bennett, A. K. (1993). Temperature, muscle power output and limitations on burst locomotor performance of the lizard Diposaurus dorsalis. *J. Exp. Biol.* **174**, 185-197.

Tidball, J. G. and Daniel, T. L. (1986). Elastic energy storage in rigored skeletal muscle cells under physiological loading conditions. *Am. J. Physiol.* **250**, R56-64.

Tu, M. S. and Daniel, T. L. (2004a). Cardiac-like behavior of an insect flight muscle. *J. Exp. Biol.* **207**, 2455-2464.

Tu, M. S. and Daniel, T. L. (2004b). Submaximal power output from the dorsolongitudinal flight muscles of the hawkmoth *Manduca sexta. J. Exp. Biol.* **207**, 4651-62.

Tu, M. and Dickinson, M. (1994). Modulation of Negative Work Output From a Steering Muscle of the Blowfly Calliphora Vicina. *J. Exp. Biol.* **192**, 207-24.

Wakeling, J. M. (2009). The recruitment of different compartments within a muscle depends on the mechanics of the movement. *Biol. Lett*. **5**, 30-4.

Walker, S. M. and Schrodt, G. R. (1974). I segment lengths and thin filament periods in skeletal muscle fibers of the Rhesus monkey and the human. *Anat. Rec.* **178**, 63-81.

Wang, L. C. and Kernell, D. (2001). Fibre type regionalisation in lower hindlimb muscles of rabbit, rat and mouse: a comparative study. *J. Anat.*, **199**, 631-43.

Wojdyr, M. (2010). Fityk : a general-purpose peak fitting program. *J. App. Crystal.* **43**, 1126-1128.

Wu, J. and Sun, M. (2005). Unsteady aerodynamic forces and power requirements of a bumblebee in forward flight. *Acta Mech.* **21**, 207-217.

Yu, L. C., Steven, A. C., Naylor, G. R. S., Gamble, R. C., and Podolsky, R. J. (1985). Distribution of mass in relaxed frog skeletal muscle and its redistribution upon activation. *Biophys. J.* **47**, 311-321.

Appendix A

MATLAB CODE FOR CHAPTER 2

```
% Code to analyze rise and fall times of contraction

signal = b(:,3);
samprate = 5000;
lfro=1;
hfro=200;
fs=5e3;
opt=0;
newsignal = bandpass2(signal,lfro, hfro, fs, opt);

plot(newsignal);


%% make matrix of multiple points, then use a for loop on the
outside.
[x y] = ginput(10);
x=round(x);

a1=newsignal(x(1):x(2));
b1=newsignal(x(3): x(4));
c1=newsignal(x(5): x(6));
d1=newsignal(x(7): x(8));
e1=newsignal(x(9): x(10));

new_data=NaN(6000,5);

new_data(1:length(a1),1)=a1;
new_data(1:length(b1),2)=b1;
new_data(1:length(c1),3)=c1;
new_data(1:length(d1),4)=d1;
new_data(1:length(e1),5)=e1;

risetime_compiled=[];
falltime_compiled=[];
maximumF_compiled=[];

for i=1:length(new_data(1,:));
```

```
    maxF = max(new_data(:,i));
    baseF = mean(new_data(1:20,i));
    lowF = (maxF-baseF)*0.1;


    peaktimeindx = find(maxF == new_data, 1, 'first' );
    i2 = peaktimeindx;
    while new_data(i2) - baseF > lowF;
        i2 = i2-1;
    end
    upindx = i2 ;

    i2 = peaktimeindx+4;
    while new_data(i2) -baseF > lowF;
        i2 = i2+1;
    end
    downindx = i2;

    risetime = (peaktimeindx - upindx)/5000;
    falltime = (downindx - peaktimeindx)/5000;
    maximumF = maxF - baseF;


    risetime_compiled(:,i)=risetime;
    falltime_compiled(:,i)=falltime;
    maximumF_compiled(:,i)=maximumF;

end;

  Rise=risetime_compiled';
  Fall=falltime_compiled';
  Force= maximumF_compiled';
  contraction_dynamics=[Rise Fall Force];

  mean_rise = median(Rise);
  sd_rise= std(Rise)
  mean_fall= median(Fall);
  sd_fall= std(Fall);
  mean_maxF= median(Force);
  sd_maxF= std(Force)

  contra_dyn_single_twitch=[Rise  Fall  Force ];

  rise_stats=[mean_rise sd_rise]';
  fall_stats=[mean_fall sd_fall]';
  force_stats=[mean_maxF sd_maxF]';
  contra_dyn_single_twitch_stats = [ rise_stats fall_stats
```

```
force_stats ]


save 40a contra_dyn_single_twitch
contra_dyn_single_twitch_stats
```

Appendix B

MATLAB CODE TO RUN WORK-LOOP EXPERIMENT (CHAPTER 3 AND 4)

```
% Work loops: measure force, length, stim
%2010_11_30 now records motor force output

%% set up DAQ board output: Large NI DAQ
clear all

% detect and initialize the A/D equipment: large daq first
try
  hw = daqhwinfo('nidaq');
  for i=1:length(hw)
    j = strcmp('USB-6229',hw(i).BoardNames);
    if j(1) == 1
      adDevice=hw(i).InstalledBoardIds;
    end
  end
catch
   disp('DAQ not connected')
%   return
end
%=============================================================
=========

%Set up output for large daq
ao = analogoutput('nidaq', 'Dev1'); % open DAQ
addchannel(ao, 0); % sine wave for motor
addchannel(ao, 1); % stim signal for stimulator

SampleRate=5000;

%ao.SampleRate = 5000;

set(ao,'SampleRate',SampleRate);
ActualRate = get(ao,'SampleRate')
```

```
%set(ao,'SamplesPerTrigger',duration*SampleRate);

set(ao,'TriggerType', 'Immediate');

%ao.TriggerType='Immediate';
%ao.RepeatOutput = manual;
DAQObj.ao = ao; % put the ao object into DAQ structure


%% set up DAQ board input: large daq
    ai = analoginput('nidaq', 'Dev1'); % open DAQ
    addchannel(ai, (0:3));
    ai.SampleRate = 5000; %Enter sample rate for input, was at
10 samples per second
    ai.TriggerType='Immediate';
    ai.TriggerRepeat = inf; % set to infinite, otherwise it
only aquires 1000pts for each repeat
    set(ai, 'LoggingMode', 'Disk&Memory');

    LogFileIndex = datestr(now,30); % call a timestamp
routine...
    LogFileName = ['recording_' LogFileIndex];


%% SET UP OUTPUT SIGNAL

f_sampling = 5000; % output sampling rate in Hz
trial_duration = 4; % in seconds
time = 0:1/f_sampling:trial_duration; % create time vector

%Parameter for the phase of activation (stim)
%want phase of activation=0.36 0.49 0.58
%play around with the numbers during beginning of experiment
to get the phases of activation you want
%for each different trial I select a different phase of
activation

%k= 0.44*pi;  %was 0.2: for phase 0.28
%k= 0.66*pi   %was 0.55: for phase 0.46
k= 0.8*pi;    %for phase 0.58

sine_amp = 0.75; sine_freq = 25; sine_phase = 0; % parameters
for the sine wave
sine_signal = sine_amp * sin(2*pi*time*sine_freq -
sine_phase); % create sinusoid
sine_signal = ( sine_signal + sine_amp ) / 2; % scale the
signal to go from 0 to 5 (Volts)
sine_signal = sine_signal(:); % create column vector so it
```

```
fits into DAQ output matrix later
new_sine_signal=ones(15000,1);
new_sine_signal2=(sine_amp*new_sine_signal)/2;
new_sine_signal3=new_sine_signal2;% can't figure out why i
used these steps, sorry :(
new_sine_signal3(1:length(sine_signal),1)=sine_signal;


% Create pulse signal at sine wave frequency:
pulse_phase = k;  % loop counter sets phase.
pulse_dutycycle = sine_freq ; % change duty cycle to get a
fatter or less fat pulse
% create the pulse signal w/ same frequency as sine above:
pulse_signal = square(2*pi*sine_freq*time - pulse_phase,
pulse_dutycycle);
pulse_signal = 5 * ((pulse_signal+1) / 2); % scale it to go
from 0 to 5 Volts (TTL signal)
pulse_signal = pulse_signal(:);
new_pulse_signal=zeros(15000,1);
new_pulse_signal(1:length(pulse_signal),1)=pulse_signal;

putdata(DAQObj.ao, [new_sine_signal3  new_pulse_signal ]);

%% Start DAQ boards
      start(ai); % start the analog in
      start(DAQObj.ao);

      fprintf('\n\nRecording.... Press button to stop data
acquisition\n\n');
      pause;
      [ChData, t] = getdata(ai, ai.SamplesAcquired);
      stop(ai); % will stop when you press a button on the
comp.
      stop(DAQObj.ao);


%% Record Input

    %Ch1= Force, Ch2=EMG, Ch3=Length Ch4=X-ray shutter signal

% FORCE
    %Find NaN and eliminate them by finding the average value
of their neighbor and substitute
    ndx_NaN=find(isnan(ChData(:,1)));
    new_voltage=ChData(:,1);
    new_voltage(ndx_NaN)=(new_voltage(ndx_NaN-
1)+new_voltage(ndx_NaN+1))/2;
```

```
    force_voltagediff= new_voltage(:,1) - new_voltage(1,1);

    %Calibrate force and length manually by hanging weights
off the force
    %transducer of moving the motor lever arm by known
amounts.

    %Calibrate voltage to force:
    Force=1.3986*force_voltagediff;% for trials July 15 2010
and later
    F=Force;
    cForce_length=0.00006*force_voltagediff;  %length change
the force transducer undergoes

% LENGTH

    %Find NaN and eliminate them by finding the average value
of their neighbor and substitute
    ndx2_NaN=find(isnan(ChData(:,3)));
    new_voltage2=ChData(:,3);
    new_voltage2(ndx2_NaN)=(new_voltage2(ndx2_NaN-
1)+new_voltage2(ndx2_NaN+1))/2;

    %ndx_NaN=find(isnan(c))
    length_voltagediff= new_voltage2(:,1) - new_voltage2(1,1);
    Length = length_voltagediff*0.0008581*-1;
    L=Length;
    deltaL=cForce_length + Length; %ultimate length including
the
    %length change caused by the bending force transducer

  %% Matrix 'b' contains all information
  b = [t ChData(:,1) F ChData(:,3) L deltaL ChData(:,2)
ChData(:,4)];
  %b(:,1)=time
  %b(:,2)=force transducer output
  %b(:,3)=calibrated force signal
  %b(:,4)=  length
  %b(:,5)= calibrated length
  %b(:,6)= delta length
  %b(:,7)= stim
  %b(:,8)=xray shutter

fprintf('Saved result matrix as: %s \n\n', LogFileName);

save(LogFileName, 'b', 'F', 'deltaL' );
```

Appendix C

MATLAB CODE TO ANALYZE WORK-LOOP DATA (CHAPTER 3 AND 4)

```
% To calculate work done for all the files in a folder
% Pre analyze the data in Centipede3. to pull out specific
time points
%including EMG times, min length time (keeping in mind with
work-loops we consider positive length
%to be in the shortening direction for max positive length
recorded is actually when
%the muscle is shortest)
clear all

% Firt Pull the .data files that correspond to the data you
want
if exist('dataDir')~=1 %If you haven't already picked a
directory,
      dataDir = uigetdir(pwd, 'Select the data directory');
%go get the folder your data is in.
  end


% get a list of data files in dataDir
dataFiles=dir([dataDir,'/filteredrecording_*.mat']);
%This variable has all of the data files in it with a .mat
extension.

%Set mass of muscle to get mass specific power output (g):
m=0.1859
nm=[];

for i=1:length(dataFiles); %Go through the data files
    fname=dataFiles(i).name; %Get their names
    nm = fname(1:length(fname)-4); %Take the extension off the
name

  try
    sortfile = [nm,'Data.out']; %Look for the sorted file to
match the .mat file
```

```
      sorteddata = importdata([dataDir,filesep, sortfile]);
%Get the data from that sorted file
  catch sorteddata.data = [0 0 0 0]; %If there is no sorted
file, fill in with zeros
  end

    data = sorteddata.data; %Pull the sorted data out of the
struct
    %raw=importdata([dataDir,filesep,fname]); %Get the raw
data from the .mat file
    load(nm);
    %Now you have the raw data (raw) and the sorted data
(data). In this
    %space, you can do what ever calculations you want and
save them.
    mlt(:,1)=data(10:31,1) ; %pull out times when muscle
starts to lengthen,
    %start with the 10th cycle to avoid bad motor movement
    stim_time(:,1)= data(10:31,3);
    %now you have a vector of the stim and min length times
you selected
    %with Centipede3

    %to calculate phase of activation
    phase_compiled=[];
   for i=1:20;
     phase = [stim_time(i+1)-mlt(i)]/[mlt(i+1)-mlt(i)];
     phase_compiled(i,1)=phase;
   end
    mean_phase=mean(phase_compiled);

    %Find index# of stim_times
    %first average the signal a little to match the signal
values with the stim_time values
    btestr=round(b(:,1)*10000);
    btestr=btestr./10000;
    stimindx_compiled=[];
    for i=1:length(stim_time(:,1));
        stimindx = find(stim_time(i,1) == btestr);
        stimindx_compiled(i,1)=stimindx;
    end
    si=stimindx_compiled;

    %If the force signal needs to be filtered:
%     signal = b(:,3);
%     samprate = 5000;
%     lfro=1;
```

```
%     hfro=100;
%     fs=5e3;
%     opt=0;
%     Fnewsignal = bandpass2(signal,lfro, hfro, fs, opt);

   %break it into 20 cycles
    fsignal=b(:,3) ;   %=Fnewsignal;
    force=NaN(250,20);
    for i=1:20;
        indxlength=si(i+1)-si(i);
        indxlength2=indxlength+1;
        force(1:indxlength2,i)=fsignal(si(i):si(i+1));
    end

%If the length signal needs to be filtered:
%     signal = b(:,6);
%     samprate = 5000;
%     lfro=1;
%     hfro=100;
%     fs=5e3;
%     opt=0;
%     Lnewsignal = bandpass2(signal,lfro, hfro, fs, opt);

    %break it into 20 cycles
    lsignal = b(:,6);  %=Lnewsignal;
    length1=NaN(250,20);
    for i=1:20;
        indxlength=si(i+1)-si(i);
        indxlength2=indxlength+1;
        length1(1:indxlength2,i)=lsignal(si(i):si(i+1));
    end

    %Now Analyze the Length and Force Data for Work-Loops
    %And get strain
    net_work_compiled=[];
    strain=[];
    workin_compiled=[];
    workout_compiled=[];

    for i=1:20
        force2=force(:,i);
        force2_withoutNaN=force2(~isnan(force2));

        length2=length1(:,i);
        length2_withoutNaN=length2(~isnan(length2));
        dx = diff(length2_withoutNaN);

        strain(:,i)=max(length2_withoutNaN)-
```

```
min(length2_withoutNaN);

        Fa=force2_withoutNaN(1:end-1,1);
        Fb=force2_withoutNaN(2:end,1);
        W=dx.*(Fa+Fb)/2;
        net_work=sum(W);
        net_work_compiled(:,i)=net_work;

        pWi = find(W>0);  % Index into x, F, or W of positive
work
        nWi = find(W<0);  % Index into x, F, or W of negative
work
        % index for when shortening or lengthening
        posdxi=find(dx>0);  %shortening
        negdxi=find(dx<0);  %lengthening
        Win=abs(sum(W(negdxi)));
        Wout=sum(W(posdxi));
        workin_compiled(:,i)=Win;
        workout_compiled(:,i)=Wout;
     end;

     mean_strain=mean(strain);

     % final data set:
     strain=strain';
     workin_compiled=workin_compiled';
     workout_compiled=workout_compiled';
     net_work_compiled=net_work_compiled';
     mean_net_work=mean(net_work_compiled);
     sd_net_work=std(net_work_compiled);
     work_stats=[mean_net_work sd_net_work];
     power_per_kg=mean_net_work*25/(m/1000)
     power_compiled=net_work_compiled*25/(m/1000);
     compiled20=[strain phase_compiled workin_compiled
workout_compiled net_work_compiled power_compiled];
     name=[nm,'analyzed'];

     save(name, 'compiled20', 'mean_phase',
'mean_net_work','work_stats','power_per_kg', 'b',
'mean_strain') ;

%Figure with the x-axis as Length
     F=force2;
     x=length2*-1; %(convert it back to the perspective of the
motor, lengthening is positive)
     % Work Done at each point
     dx = diff(x);
     Fa = F(1:end-1);
```

```
     Fb = F(2:end);
     W = dx.*(Fa+Fb)/2;
     %dx will either be positive(muscle is lengthening) or
negative (muscle is shortening)
     % Separate Work in, Work out
     pWi = find(W>0);  % Index into x, F, or W of positive
work
     nWi = find(W<0);  % Index into x, F, or W of negative
work
     % index for when shortening or lengthening
     posdxi=find(dx>0);  %shortening
     negdxi=find(dx<0);  %lengthening

     Win=abs(sum(W(negdxi)));
     Wout=sum(W(posdxi));

     %work out is shortening since greater work out leads to a
+. The amount of
     %work put in should be less than the amount that comes
out for it to be
     %positive work.

     mx = mean(x);
     mdF = mean(F);
     fig=2;

     if fig;
        h=figure(fig);clf;hold on;
        plot(x,F,'k')
        plot(x(pWi)+dx(pWi)/2,(Fa(pWi)+Fb(pWi))/2,'r.'); %red
for positive
        plot(x(nWi)+dx(nWi)/2,(Fa(nWi)+Fb(nWi))/2,'b.'); %blue
for negative
        xlabel('Length (m)');ylabel('Force (N)');
     if Win < Wout
        text(mx,mdF,'+','FontSize',40)
     else
        text(mx,mdF,'-','FontSize',26)
     end
     end

     saveas(h, nm, 'epsc')

end

% get a list of data files in dataDir
dataFiles=dir([dataDir,'/*analyzed.mat']);
%This variable has all of the data files in it with a .mat
```

```
extension.

results=cell(24,4);

for i=1:length(dataFiles); %Go through the data files
    fname=dataFiles(i).name; %Get their names
    nm = fname(1:length(fname)-4) %Take the extension off the
name

    load(nm)
    %Now you have the raw data (raw) and the sorted data
(data). In this
    %space, you can do what ever calculations you want and
save them.

    results2=num2cell(results);
    results{i,1}=nm;
    results{i,2}=mean_strain(1,1);
    results{i,3}=mean_phase(1,1);
    results{i,4}=mean_net_work(1,1);
    results{i,5}=work_stats(1,2);
    results{i,6}=power_per_kg(1,1);

end

save compiled_results.mat results
```

VITA

Nicole George was born and raised in Nairobi, Kenya. Those years spent exploring the wildlife-rich savannah with her family solidified a passion for the natural world early on. When Nicole was awarded a book on dinosaurs in the second grade, naturally she decided to become a Paleontologist. This then transitioned into a dream to become an Astronaut, a Marine Biologist and then a Physiologist, all before she was even 14 years old. When attending college at the University of California, Berkeley she continued her love of science by majoring in Integrative Biology. While at UCB, by chance Nicole enrolled in a thought provoking class taught by Dr. Mimi Koehl and Dr. Bob Full, which brought the exciting field of biomechanics into light. From there she was hooked, and after several twits and turns, Nicole eventually landed at the welcoming door of the Daniel Lab at the University of Washington, where her days soon became filled with muscle physiology experiments and migraine-inducing code writing days. It is rumored that she quite enjoyed those days.